Extracellular signal-regulated kinase (ERK) is one of the mitogen-activated protein kinases (MAPKs) that ubiquitously phosphorylate proline-directed serine/threonine residues and participate in signal transduction pathways controlling intracellular events (4, 14, 25). ERK governs mainly proliferation, differentiation, and cell survival through being activated by a wide range of cytokine and growth factor stimuli. Several nuclear transcription factors have been identified as in vivo substrates for MAPKs, molecular functions of which are altered through phosphorylation. TEL is also a nuclear phosphoprotein that possesses multiple putative MAPK phosphorylation sites (26). However, the functional significance of the phosphorylation has not yet been elucidated. In the present study, we investigated the regulation of TEL's functions through ERK-induced phosphorylation. TEL became phosphorylated by ERK on two serine residues, Ser^{213} and Ser^{257}, in the internal domain between the HLH and ETS domains. TEL lost its abilities to repress transcription through the phosphorylation. A glutamate mutant molecularly mimicking hyperphosphorylated TEL also completely blocked TEL-mediated erythroid differentiation in MEL cells and antagonized TEL-induced growth suppression in H-Ras-transformed NIH 3T3 cells. Importantly, endogenous TEL proteins were found to be dephosphorylated in parallel with ERK inactivation during erythroid differentiation in MEL cells and to be phosphorylated by activated ERK in H-Ras-transformed NIH 3T3 cells. These results suggest that TEL's biological functions could be physiologically regulated through ERK-induced phosphorylation via various differentiation and proliferation signals.

MATERIALS AND METHODS

Plasmid construction. pME18S-FLAG-TEL, pCXN2-FLAG-TEL, pME18S-FLAG-ΔHLH-TEL, pME18S-FLAG-Δ5′ID-TEL, pME18S-FLAG-ΔETS-TEL, pME18S-FLAG-ΔHLH+5′ID-TEL, pME18S-FLAG-ΔHLH+ID-TEL, and pME18S-EVI-1 were described previously (1, 33). The TEL mutants S22, S213, S238, and S257 were obtained by leaving the serine residues of the amino acids indicated and replacing the remaining residues among Ser^{22}, Ser^{213}, Ser^{238}, and Ser^{257} with alanines in pME18S-FLAG-TEL by using the Chameleon double-stranded site-directed mutagenesis kit (Stratagene). The TEL mutants E22, E213, E238, E257, E213/238, E238/257, E213/257, E22/257, E22/213/257, and E213/238/257 were also obtained by replacing the serine residues of the amino acids indicated with glutamates in pME18S-FLAG-TEL. Both FLAG-tagged wild-type TEL and E213/257 mutant cDNAs were cloned into the EcoRI site of pCDNA3 (Invitrogen) and pSRαMSVtkneo retrovirus vector. FLAG-tagged wild-type TEL and S22, S213, S238, and S257 mutant cDNAs were cloned into the EcoRI site of pGEX-1 (Pharmacia). FLAG-tagged E213/257 mutant and influenza virus hemagglutinin (HA)-tagged wild-type TEL cDNAs were also cloned into the EcoRI site of the pCXN2 and the pCAGIpuro expression plasmids that carry the neo^R and the $puromycin^R$ genes, respectively. pCMVMK, which is an expression vector of a rat ERK1-ERK2 chimeric protein, was described previously (31). To construct ERK-ΔCD, two Aor51HI sites (positions 915 and 996) were created by means of site-directed mutagenesis and the internal fragment from mutagenic Aor51HI (position 915) to mutagenic Aor41HI (position 996) was deleted. Activated H-Ras genomic DNA was purchased from JCRB GenBank and was cloned into the pCAGIPuro expression plasmid. The pGL2-754TR reporter plasmid contains a natural promoter derived from the *stromelysin-1* gene (6).

Cell culture. A Friend virus-induced erythroleukemia cell line, MEL-B8, and NIH 3T3 and COS-7 cells were maintained in Dulbecco's modified Eagle's medium (DMEM) supplemented with 10% fetal calf serum (FCS). To activate ERK, COS-7 cells were treated with 10% FCS plus 100 ng of recombinant human epidermal growth factor (EGF; Wakunaga) per ml after serum starvation with 0.1% FCS. To induce erythroid differentiation in MEL cells, 5 mM HMBA (Sigma-Aldrich) was added to the culture. Erythroid differentiation was determined by calculating the percentage of hemoglobin-producing cells following benzidine staining.

Isolation of stable transfectants. To establish stable transfectants of wild-type TEL or the E213/257 mutant, 1×10^7 MEL cells were electroporated with 20 μg of each cDNA cloned into the pCXN2 plasmid at 380 V and 975 μF by using Gene Pulser (Bio-Rad). Transfected cells were selected with 0.8 mg of G418 (Sigma-Aldrich)/ml and cloned by limiting dilution. Survival clones were screened for the expression of wild-type TEL or the E213/257 mutant by Western analysis with anti-FLAG M2 antibody (Sigma-Aldrich). To further obtain double transfectants of the wild-type-TEL and the E213/257 mutant, 2×10^6 MEL cells stably expressing the E213/257 mutant were electroporated with 8 μg of wild-type TEL cDNA cloned into the pCAGIpuro plasmid at 500 V and 25 μF by using Gene Pulser. Electroporated cells were selected with 0.75 μg of puromycin (Sigma-Aldrich)/ml and cloned by limiting dilution. Survival clones were screened for concomitant expression of the wild-type TEL and the E213/257 mutant by Western analysis with anti-HA (BAbCO) and anti-FLAG M2 antibodies. To establish stable transfectants expressing the activated H-Ras mutant, 5×10^5 NIH 3T3 cells were transfected with 10 μg of the pCAGIPuro-H-Ras expression plasmid by the Lipofectin method with TransFast (Promega). Transfected cells were selected with 0.3 μg of puromycin/ml and cloned by limiting dilution. Survival clones were screened for the expression of H-Ras by Western analysis with anti-H-Ras F235 antibody (Santa Cruz Biotechnology).

Western analysis and immunoprecipitation. COS-7 cells were transfected with FLAG-tagged wild-type TEL or its mutant expression plasmids alone or in combination with ERK expression plasmid by the DEAE-dextran method as described previously (33). Western analyses were performed as described previously (22) by using anti-FLAG M2, anti-HA, anti-ERK1 C-16 (Santa Cruz Biotechnology), or anti-phosphorylated ERK E10 (New England BioLabs) antibody. The blots were visualized by using the Problot AP system (Promega). Immunoprecipitation was carried out with anti-FLAG M2 or anti-TEL N-19 (Santa Cruz Biotechnology) antibody conjugated with protein G-Sepharose (Pharmacia), and immunoprecipitates were analyzed by sodium dodecyl sulfate-polyacrylamide gel electrophoresis (SDS-PAGE).

Metabolic labeling. COS-7 cells were cultured for 36 h after transfection in DMEM containing 10% FCS, transferred to DMEM containing 0.1% FCS, and incubated for 12 h. They were then transferred and cultured for 3 to 4 h in methionine- or phosphate-free DMEM supplemented with 0.1% FCS (dialyzed against 150 mM NaCl) plus 100 μCi of [^{35}S]methionine (Tran-^{35}S label; ICN)/ml or 400 μCi of [^{32}P]orthophosphate (Phosphorus-32; Amersham)/ml. Then, they were either left untreated or treated with 10% FCS (dialyzed against 150 mM NaCl) plus 100 ng of recombinant human EGF per ml for 5 min.

Parental MEL cells were cultured in DMEM containing 10% FCS with 5 mM HMBA for the indicated periods and were then transferred and cultured for 12 h in methionine- or phosphate-free DMEM supplemented with 10% FCS (dialyzed against 150 mM NaCl) plus 100 μCi of [^{35}S]methionine/ml or 400 μCi of [^{32}P]orthophosphate/ml.

After incubation in DMEM containing 10% FCS for 36 h, nontransformed or H-Ras-transformed NIH 3T3 clones were transferred and cultured for 12 h in methionine- or phosphate-free DMEM without FCS but with 100 μCi of [^{35}S]methionine/ml or 400 μCi of [^{32}P]orthophosphate/ml.

In vitro kinase and pull-down assays. Glutathione *S*-transferase (GST)-wild-type-TEL, S22, S213, S238, and S257 proteins were produced as described previously (17). For an in vitro kinase assay, COS-7 cells that were transfected with ERK expression plasmid were stimulated with EGF as described above. Cell lysates were immunoprecipitated with anti-ERK1 antibody conjugated with protein G-Sepharose and subjected to an in vitro kinase reaction with myelin basic proteins (MBPs) (Sigma-Aldrich) or GST-wild-type-TEL, S22, S213, S238, and S257 fusion proteins as a substrate as described previously (1). A pull-down assay was performed with GST-wild-type-TEL and COS-7 lysates expressing ERK or ERK-ΔCD as described previously (1).

Luciferase assay. NIH 3T3 cells were transfected with 1 μg of the pGL2-754TR reporter plasmid alone or along with 1 μg of expression plasmids by using TransFast (Promega). Luciferase assays were performed using the Dual-Luciferase reporter assay system (Promega) as described previously (1). We confirmed that all of the proteins used in this study were expressed at almost similar levels (data not shown).

EMSA. COS-7 cells were transfected with TEL expression plasmid alone or along with ERK expression plasmid and either left untreated or treated with EGF. Wild-type TEL and E213/257 mutant proteins were in vitro translated with pCDNA3 expression plasmids by using the TNT coupled wheat germ extract system (Promega). The procedures for the electrophoretic mobility shift assay (EMSA) and the oligonucleotides used were reported previously (33).

Viral infection. To prepare the retrovirus stocks, 10 μg of pSRαMSVtkneo, pSRαMSVtkneo-TEL, or pSRαMSVtkneo-E213/257 construct was transfected with 40 μg of ψ packaging plasmid into 1×10^6 COS-7 cells by the DEAE-

dextran method. The culture medium containing viruses was harvested 96 h after transfection. Viral titers were determined and normalized. Viral infections were carried out by exposing 5×10^4 H-Ras-transformed NIH 3T3 cells to 1 ml of virus stocks for 8 h. G418-resistant populations were selected in medium containing 0.4 mg of G418/ml after additional incubation for 48 h in medium without G418. The following experiments were performed with uncloned cell populations.

Transformation assay. For a soft agar assay, cells of each transfected derivative were trypsinized, suspended in DMEM containing 0.3% agar and 20% FCS, and plated onto a bottom layer containing 0.6% agar. Cells were plated at a density of 2×10^4 cells/3.5-cm dish in quadruplicate, and colonies >0.125 mm in diameter were enumerated after 14 days. The numbers of colonies are presented as mean values.

RESULTS

TEL is phosphorylated in vivo with dependence on activation of ERK. MAPK-induced phosphorylation of several transcription factors is frequently detected as size-shifted bands of the proteins with SDS-PAGE (30). To clarify a role of TEL in the Ras/ERK signaling pathways, we examined whether TEL becomes phosphorylated through the activation of ERK. We observed three differently migrating bands (two slow-migrating bands and one fast-migrating band) derived from TEL in Western analysis, when TEL expression plasmid was introduced into COS-7 cells (Fig. 1A). Interestingly, overexpressed TEL showed a size shift when COS-7 cells cotransfected with ERK expression plasmid were serum starved and stimulated with EGF. Then, kinase activities of endogenous or overexpressed ERK in COS-7 cells were evaluated by an in vitro kinase assay with immunoprecipitates with anti-ERK antibody and its known substrate MBP (Fig. 1B). Endogenous ERK was slightly activated upon EGF stimulation, as judged by the phosphorylation status of MBP. The most prominent ERK activity was detected when ERK-transfected COS-7 cells were treated with EGF. We thus concluded that the EGF treatment potentiated kinase activities of overexpressed ERK in COS-7 cells. Therefore, TEL seems to be phosphorylated through the activation of ERK. To confirm in vivo phosphorylation of TEL proteins by activated ERK, we next employed [^{35}S]methionine and [^{32}P]orthophosphate labeling. FLAG-tagged TEL was transiently expressed with or without overexpressed ERK in COS-7 cells and immunoprecipitated with anti-FLAG antibody. With [^{35}S]methionine labeling, we observed two TEL-derived bands (a broad slow-migrating band and a narrow fast-migrating band) when only TEL was overexpressed (Fig. 1C). We also detected size-shifted bands when cotransfected ERK was stimulated with EGF. When [^{32}P]orthophosphate labeling was carried out, the former slow- and fast-migrating bands turned out to be derived from phosphorylated and unphosphorylated forms of TEL, respectively. The latter shifted bands appeared to be derived from hyperphosphorylated forms. These data indicate that approximately two-thirds of overexpressed TEL molecules are constitutively phosphorylated and that almost all of them are inducibly hyperphosphorylated upon ERK activation.

ERK-dependent phosphorylation at Ser^{257} is detectable as a size shift. Overexpressed TEL proteins were detected as three differently migrating bands in COS-7 cells by Western analysis (Fig. 1A). In contrast to the results of the [^{35}S]methionine- and [^{32}P]orthophosphate-labeling experiments, two slow-migrating bands were considered to be derived from phosphorylated

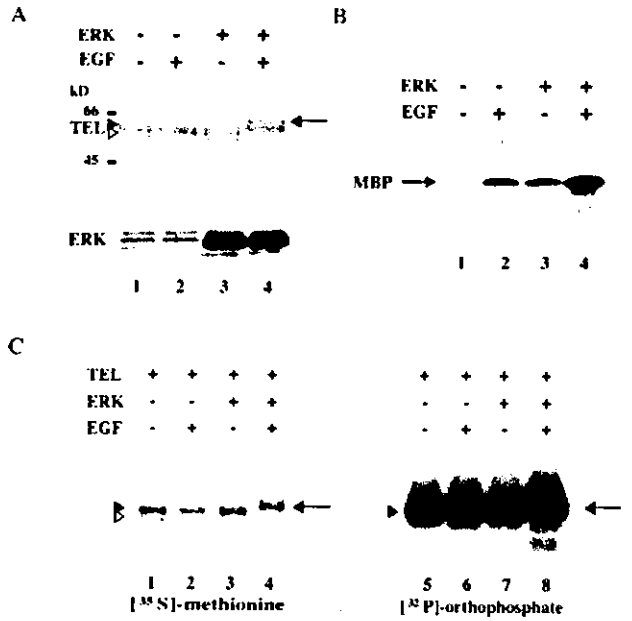

FIG. 1. (A) TEL shows a size shift upon activation of ERK. COS-7 cells were transfected with 5 μg of pME18S-FLAG-TEL alone (lanes 1 and 2) or together with 5 μg of pCMVMK (ERK expression plasmid) (lanes 3 and 4), starved in medium containing 0.1% FCS, and either left untreated (lanes 1 and 3) or treated with recombinant human EGF for 5 min (lanes 2 and 4). Western analyses were performed with anti-FLAG or anti-ERK1 antibody. (B) ERK activities in COS-7 cells. COS-7 cells were not transfected (lanes 1 and 2) or transfected with 5 μg of ERK expression plasmid (lanes 3 and 4) and treated as described for panel A. In vitro kinase assays were performed with MBP as a substrate. (C) [^{35}S]methionine and [^{32}P]orthophosphate labeling of TEL proteins. COS-7 cells were transfected with 5 μg of pME18S-FLAG-TEL alone (lanes 1, 2, 5, and 6) or together with 5 μg of ERK expression plasmid (lanes 3, 4, 7, and 8), subjected to metabolic labeling with [^{35}S]methionine (lanes 1 to 4) or [^{32}P]orthophosphate (lanes 5 to 8), treated as described for panel A, and immunoprecipitated with anti-FLAG antibody. Open arrowheads, solid arrowheads and solid arrows in panels A and C indicate unphosphorylated, phosphorylated, and hyperphosphorylated forms of TEL, respectively. Positions of size markers (in kilodaltons) are shown.

forms and a fast-migrating band was considered to be derived from unphosphorylated forms. The retarded bands that were observed when exogenous ERK was activated mirrored those of hyperphosphorylated forms. In order to determine phosphorylation sites in TEL, a set of deletion mutants (shown in Fig. 2A) were expressed with ERK in COS-7 cells and subsequently analyzed for size shifts after the EGF stimulation with SDS-PAGE. When three types of TEL mutants (ΔHLH-TEL, ΔHLH+5′ID-TEL, and ΔETS-TEL) were expressed in the presence of activated ERK, retarded bands were induced with almost the same pattern as in wild-type TEL (Fig. 2B). However, we did not detect such a size shift by ERK when ΔHLH+ID-TEL and Δ5′ID-TEL were expressed. These data suggest that major ERK-dependent phosphorylation sites exist within the region comprising amino acids 206 to 267 in TEL. We cannot completely rule out the existence of other phosphorylation sites outside this region because phosphorylation on some residues could not be detected as size shifts with SDS-PAGE.

Ser/Thr-Pro is a minimal consensus sequence for phosphor-

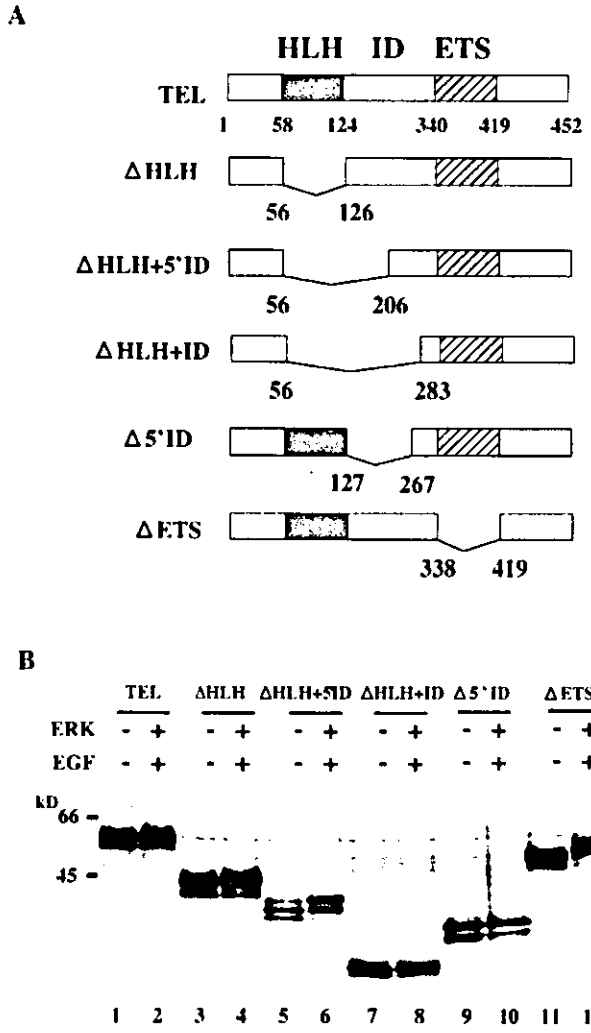

FIG. 2. (A) Structures of TEL deletion mutants. The HLH and the ETS domains are shown by shaded and hatched boxes, respectively. Numerals are amino acid numbers in the TEL protein. (B) ERK-dependent size shifts of wild-type TEL and its deletion mutants. COS-7 cells were transfected with 5 μg of pME18S-FLAG-TEL (lanes 1 and 2), pME18S-FLAG-ΔHLH-TEL (lanes 3 and 4), pME18S-FLAG-ΔHLH+5'ID-TEL (lanes 5 and 6), pME18S-FLAG-ΔHLH+ID-TEL (lanes 7 and 8), pME18S-FLAG-Δ5'ID-TEL (lanes 9 and 10), or pME18S-FLAG-ΔETS-TEL (lanes 11 and 12) alone (lanes 1, 3, 5, 7, 9, and 11) or in combination with 5 μg of ERK expression plasmid (lanes 2, 4, 6, 8, 10, and 12), serum starved, and either left untreated (lanes 1, 3, 5, 7, 9, and 11) or treated with recombinant human EGF for 5 min (lanes 2, 4, 6, 8, 10, and 12). Western analysis was performed with anti-FLAG antibody. Positions of size markers (in kilodaltons) are shown.

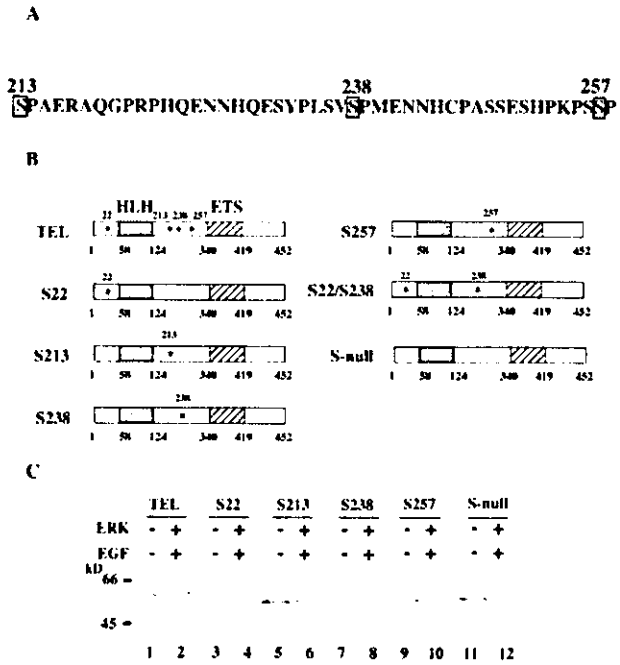

FIG. 3. (A) Potential sites of phosphorylation by ERK in TEL. Potential phosphorylation sites that meet a minimal consensus sequence (Ser/Thr-Pro) and reside within the region comprising amino acids 206 to 267 are boxed. Numerals are amino acid numbers in the TEL protein. (B) Structures of alanine mutants. The potential serine residues for phosphorylation, Ser^{22}, Ser^{213}, Ser^{238}, and Ser^{257}, were replaced with alanines. Asterisks show the positions of the residual serine residues. (C) ERK-dependent size shifts of wild-type TEL and its alanine mutants. COS-7 cells were transfected with 5 μg of pME18S-FLAG-TEL (lanes 1 and 2), pME18S-FLAG-S22 (lanes 3 and 4), pME18S-FLAG-S213 (lanes 5 and 6), pME18S-FLAG-S238 (lanes 7 and 8), pME18S-FLAG-S257 (lanes 9 and 10), or pME18S-FLAG-S-null (lanes 11 and 12) alone (lanes 1, 3, 5, 7, 9, and 11) or in combination with 5 μg of ERK expression plasmid (lanes 2, 4, 6, 8, 10, and 12) and treated as described in the legend to Fig. 2B. Western analysis was performed with anti-FLAG antibody. Positions of size markers (in kilodaltons) are shown.

ylation by all MAPKs (4). Thus, there are three potential phosphorylation sites (Ser^{213}, Ser^{238}, and Ser^{257}) within the region identified above if TEL is directly phosphorylated by ERK (Fig. 3A). Because Ser^{22} is equivalent to Thr^{38} in ETS1 and Thr^{72} in ETS2 (29), which are phosphorylated by ERK (28, 38), this serine residue is another candidate for phosphorylation by ERK. To determine whether these four candidate sites become phosphorylated depending on ERK activation, we constructed TEL mutants S22, S213, S238, and S257 by leaving each serine residue as it is and replacing the remaining three residues with alanines by in vitro mutagenesis (Fig. 3B). In addition, we also constructed S-null, in which all four serine residues were replaced by alanines. Among these mutants, only S22 showed the slow- and fast-migrating bands that might correspond to phosphorylated and unphosphorylated forms of wild-type TEL without activated ERK, while the other four mutants, S213, S238, S257, and S-null, revealed only the fast-migrating bands and were thought to remain unphosphorylated (Fig. 3C). It is conceivable that almost two thirds of overexpressed wild-type TEL molecules are constitutively phosphorylated on Ser^{22} without ERK activation. On the other hand, the S257 mutant showed the same pattern of shifted bands as wild-type TEL after ERK activation, while the remaining mutants hardly induced the shifted bands. Thus, Ser^{257} may be a major phosphorylation site depending on ERK activation, and phosphorylation at Ser^{213} and Ser^{238} is not detectable by a size shift.

TEL is directly phosphorylated by ERK in vitro at Ser^{213} and Ser^{257}. It is quite likely that TEL is directly phosphorylated by ERK, since the identified phosphorylation residue Ser^{257} meets the minimal consensus sequence for phosphorylation by

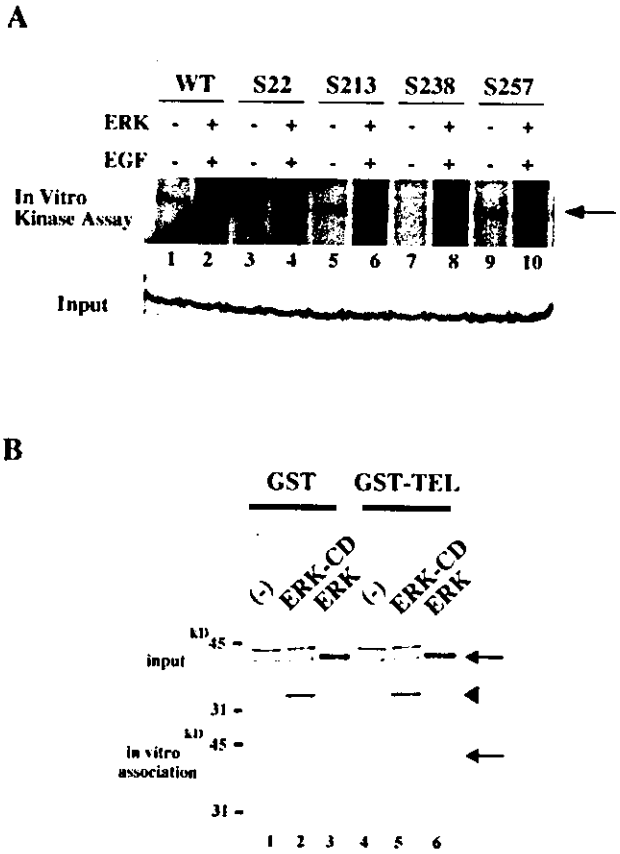

FIG. 4. (A) In vitro ERK kinase assays with wild-type TEL (WT), S22, S213, S238, and S257 as substrates. The top panel shows results of assays performed as described in the legend to Fig. 1. In the bottom panel, the input of each lane is shown by Coomassie staining. The arrow indicates GST-wild-type-TEL or its mutant fusion proteins phosphorylated by ERK. (B) Physical interaction between ERK and wild-type TEL through the CD domain in ERK. COS-7 cells were not transfected (lanes 1 and 4) or were transfected with 5 μg of ERK-ΔCD (lanes 2 and 5) or ERK (lanes 3 and 6) expression plasmid, harvested, and mixed with GST-glutathione-Sepharose beads (lanes 1 to 3) or GST-wild-type-TEL conjugated with glutathione-Sepharose beads (lanes 4 to 6). Western analyses were performed with anti-ERK antibody to detect ERK proteins expressed in COS-7 cells (top panel) and those bound to GST-wild-type-TEL (bottom panel). Arrows and a solid arrowhead indicate ERK and ERK-ΔCD proteins, respectively.

ERK. In order to confirm this possibility, a GST-wild-type-TEL fusion protein was produced in *Escherichia coli*, affinity purified, and used as a substrate for an in vitro ERK assay. ERK overexpressed in COS-7 cells was immunoprecipitated with anti-ERK antibody and subjected to the assay. GST-wild-type-TEL became phosphorylated in vitro by EGF-activated ERK (Fig. 4A). To determine phosphorylation sites in a more straightforward way, we next performed in vitro kinase assays with GST-S22, GST-S213, GST-S238, and GST-S257 fusion proteins. As expected from the Western analysis results described above, activated ERK induced phosphorylation in GST-S257 fusion protein in vitro. GST-S238 did not become phosphorylated at all, even after ERK activation, suggesting that neither Ser^{238} nor any other serine or threonine residues except Ser^{22}, Ser^{213}, and Ser^{257} are targets for ERK-induced phosphorylation. Surprisingly, GST-S213 became phosphorylated with activated ERK. This result indicates that Ser^{213} is another phosphorylation site that is not detected as a band shift with SDS-PAGE. Ser^{22}, which was considered to be a constitutive phosphorylation site on the basis of SDS-PAGE analysis, became slightly phosphorylated upon ERK stimulation as with SDS-PAGE. Taking these results together, we conclude that both Ser^{213} and Ser^{257} in TEL are ERK-inducible phosphorylation sites.

TEL physically interacts with ERK. MAPKs have been reported to physically interact with some of their substrates through their common docking (CD) domains (30, 39). Thus, we investigated whether TEL associates with ERK depending on the CD domain. For this purpose, ERK and ERK-ΔCD, which lacks the entire CD domain, were overexpressed in COS-7 cells and their associations with immobilized GST-wild-type-TEL were examined. ERK significantly associated with GST-wild-type-TEL, but ERK-ΔCD did not (Fig. 4B). We conclude that ERK phosphorylates TEL by binding to it through the CD domain.

ERK-dependent phosphorylation reduces *trans* repression by TEL. In order to obtain insights into the functional modification of TEL through ERK-induced phosphorylation, we examined whether the phosphorylation alters the *trans*-repressional abilities of TEL through EBS. We employed the pGL2-754TR reporter (6), which contains a natural promoter derived from the TEL target gene *stromelysin-1*, in luciferase assays. A twofold decrease in luciferase activities was observed when wild-type TEL was expressed (Fig. 5A). However, both coexpression of ERK and treatment with EGF attenuated transcriptional suppression by wild-type TEL (Fig. 5A and B). A mutant with substituted alanines on both Ser^{213} and Ser^{257} (S22/238) was not influenced with regard to *trans*-repressional functions by either ERK overexpression or EGF treatment. From these data, we conclude that ERK-dependent phosphorylation inhibits transcriptional repression by TEL.

We constructed a set of TEL mutants by replacing some of the four candidate serine residues for phosphorylation with glutamates that mimic phosphoserine residues. Of these mutants, only the E213/257 and E22/213/257 mutants lost their abilities to repress the transcription through the pGL2-754TR reporter and functionally mimicked ERK-induced hyperphosphorylated TEL (Fig. 5C). Therefore, we speculate that phosphorylation at both Ser^{213} and Ser^{257} is required to modify TEL's molecular functions. Moreover, coexpression of the E213/257 mutant abolished the transcriptional suppression by wild-type TEL in a dose-dependent manner (Fig. 5D). When EVI-1 was coexpressed as a control, the repression by wild-type TEL was not affected at all. These data suggest that the E213/257 mutant exerts a dominant-negative effect on TEL-mediated transcriptional inhibition. We conclude that ERK-dependent phosphorylation negatively regulates TEL's abilities as a transcriptional repressor.

ERK-dependent phosphorylation prevents DNA binding of TEL. We thus examined whether hyperphosphorylated TEL still possesses EBS-specific DNA-binding properties like unmodified TEL does. Cell lysates prepared from COS-7 cells that were transfected with the empty pME18S plasmid (mock) or unstimulated wild-type TEL- or ERK-stimulated wild-type TEL-expressing COS-7 cells were subjected to EMSA with radioactive EBS oligonucleotide as a probe. Almost the same

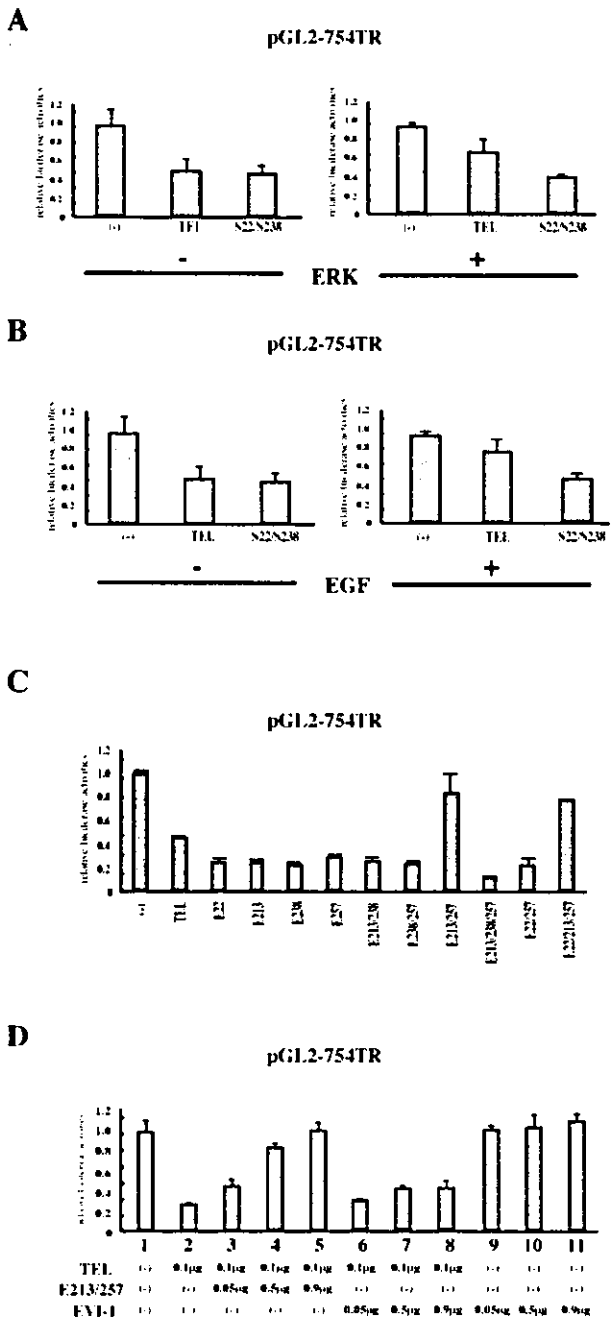

FIG. 5. (A) Overexpression of ERK inhibits TEL's *trans*-repressional ability. NIH 3T3 cells were transfected with 1 μg of the pGL2-754TR reporter plasmid alone or along with 0.5 μg of pME18S-FLAG-TEL or pME18S-FLAG-S22/S238 with or without 0.5 μg of ERK expression plasmid and cultured in DMEM containing 10% FCS for 48 h. (B) Activation of endogenous ERK also inhibits TEL's *trans*-repressional ability. NIH 3T3 cells were transfected with 1 μg of the pGL2-754TR reporter plasmid alone or along with 1 μg of pME18S-FLAG-TEL or pME18S-FLAG-S22/S238. After 48 h, the cells were incubated in DMEM containing 10% FCS with or without recombinant human EGF for 2 h before harvest. (C) Simultaneous replacement of Ser^{213} and Ser^{257} residues with glutamates eliminates TEL's *trans*-repressional ability. NIH 3T3 cells were transfected with 1 μg of the pGL2-754TR reporter plasmid alone or along with wild-type TEL or various kinds of TEL glutamate mutant expression plasmids and incubated for 48 h before harvest. (D) The glutamate mutant E213/257 shows a dominant-negative effect on TEL-mediated transcriptional repression. NIH 3T3 cells were transfected with 1 μg of the pGL2-754TR reporter plasmid alone (lane 1) or along with 0.1 μg of pME18S-FLAG-TEL (lanes 2 to 8). In lanes 3 to 8, 0.05, 0.5, and 0.9 μg of pME18S-FLAG-E213/257 or pME18S-EVI-1 were cotransfected as well. NIH 3T3 cells were also transfected with 1 μg of the pGL2-754TR reporter plasmid along with 0.05, 0.5, and 0.9 μg of pME18S-EVI-1 alone (lanes 9 to 11). Bars show luciferase activities relative to the level observed when control plasmid pME18S was cotransfected, and average results of duplicate experiments are presented.

amounts of TEL proteins were expressed in the lysates without and with ERK activation (Fig. 6A). As shown in Fig. 6A, unmodified TEL generated a specific DNA-protein complex that was supershifted with anti-TEL antibody and was hardly seen in the mock lysate. This band represented a specific binding of unmodified TEL to the EBS probe, since the binding was completely canceled by cold-specific competitors but not by nonspecific competitors. Notably, the specific DNA-protein band disappeared when TEL was hyperphosphorylated in vivo by activated ERK. These results indicate that ERK-dependent phosphorylation decreases the DNA binding of TEL.

We also compared the DNA-binding affinities of wild-type TEL and the E213/257 mutant by EMSA with in vitro-translated wild-type TEL and E213/257 mutant proteins. As shown in Fig. 6B, expression levels of wild-type TEL and E213/257 mutant proteins were almost similar. Wild-type TEL generated a specific DNA-protein complex that was completely canceled by cold-specific competitors but not by nonspecific competitors and was supershifted with two kinds of anti-TEL antibodies (N-19 and C-20). The band derived from the specific complex was quite broad, possibly because the association was extremely weak, and wild-type TEL proteins and the probe became dissociated during electrophoresis. However, the E213/257 mutant formed neither the specific DNA-protein complex nor the supershifted complex with either anti-TEL antibody. From these results, we conclude that the E213/257 mutant loses its ability for DNA binding to the EBS and conceivably mimics hyperphosphorylated TEL in DNA binding. The E213/257 mutant was found to bind to mSin3A and locate in the nucleus as wild-type TEL does (data not shown). Moreover, the glutamate mutant formed a homodimer and a heterodimer with wild-type TEL (data not shown). It could be possible that hyperphosphorylated TEL without DNA binding modulates molecular functions of nonhyperphosphorylated TEL by heterodimerizing with it.

E213/257 mutant blocks erythroid differentiation in MEL cells and stimulates growth in H-Ras-transformed NIH 3T3 cells. Considering that the E213/257 mutant has a dominant-negative effect on wild-type TEL-mediated transcriptional repression, we further analyzed alterations of TEL's biological functions through ERK-dependent phosphorylation. For this purpose, we employed MEL and NIH 3T3 cells. Because we have reported that overexpression of wild-type TEL accelerates erythroid differentiation induced by chemical compounds such as HMBA and dimethyl sulfoxide in MEL cells (33), we established clones expressing wild-type TEL, the E213/257 mutant, and both wild-type-TEL and the E213/257 mutant to test the effect of hyperphosphorylated TEL on erythroid differentiation. Figure 7A shows the expression of wild-type TEL

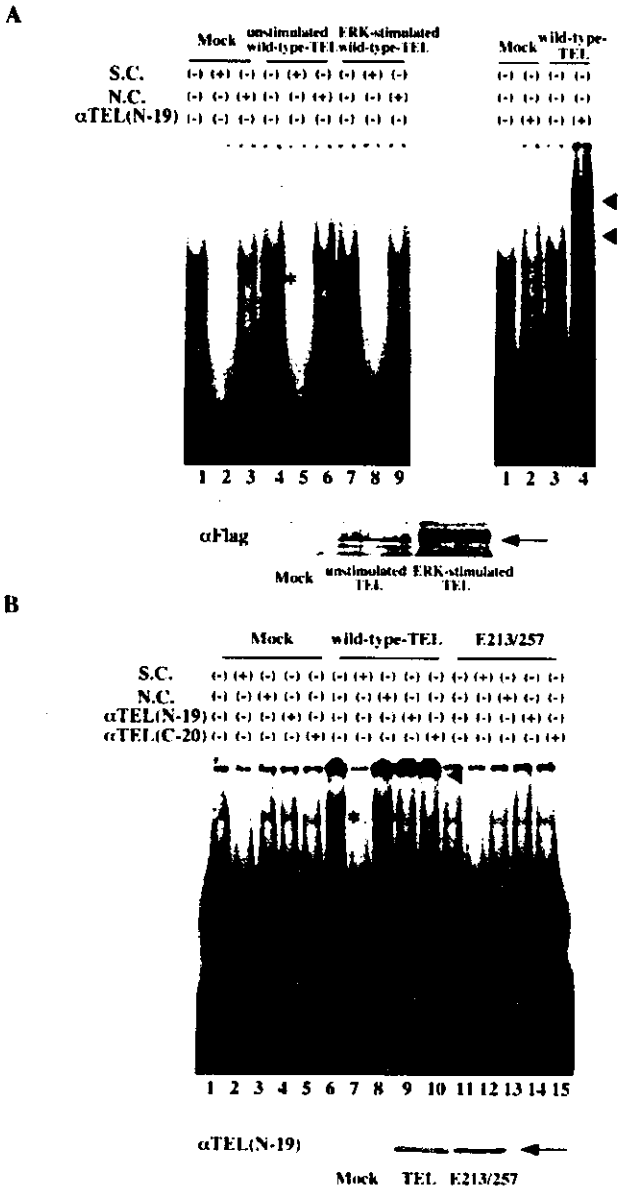

FIG. 6. (A) Hyperphosphorylated TEL does not bind to DNA. The top left panel shows results of EMSA carried out with the ^{32}P-labeled EBS probe (oligonucleotide A) and mock lysate (lanes 1 to 3), wild-type TEL-expressing COS-7 lysate without activated ERK (lanes 4 to 6), and wild-type TEL-expressing COS-7 lysate with activated ERK (lanes 7 to 9). A 300-fold molar excess of oligonucleotide A (S.C., lanes 2, 5, and 8) or oligonucleotide M (N.C., lanes 3, 6 and 9), which contains mutations in the EBS, was also added to the reaction mixtures. Asterisks indicate a specific DNA-TEL complex-derived band. The top right panel shows results obtained when anti-TEL antibody (lanes 2 and 4) was also added to the reaction mixtures. The supershifted bands are indicated with arrowheads. In the bottom panel, the expression of unstimulated or ERK-stimulated wild-type TEL protein is shown. An arrow indicates overexpressed wild-type TEL proteins. (B) The E213/257 mutant also does not bind to DNA. The top panel shows results obtained when EMSA was carried out with the ^{32}P-labeled EBS probe and mock (lanes 1 to 5), in vitro-translated wild-type TEL (lanes 6 to 10), or E213/257 (lanes 11 to 15) proteins. Asterisks indicate a specific DNA-TEL complex-derived band. A 300-fold molar excess of cold-specific competitor (S.C., lanes 2, 7, and 12) or nonspecific competitor (N.C., lanes 3, 8, and 13) was also added to the reaction mixtures. Two kinds of anti-TEL antibodies (N-19 for lanes 4, 9, and 14 and C-20 for lanes 5, 10, and 15) were added to the reaction mixtures. The supershifted bands are indicated with a solid arrowhead. In the bottom panel, the expression of in vitro-translated wild-type TEL or E213/257 protein is shown. An arrow indicates wild-type TEL or E213/257 mutant proteins.

and/or the E213/257 mutant in each of two independent clones. When stimulated with HMBA, the wild-type TEL-expressing cells showed an earlier onset and a higher incidence of benzidine positivity, while mock cells began to be benzidine positive on day 4 (Fig. 7B). Surprisingly, the E213/257-expressing cells completely lost their abilities to become benzidine positive. However, coexpression of wild-type TEL recovered E213/257 mutant-induced differentiation block. Thus, it is plausible that the dominant-negative form of TEL, namely, E213/257, blocks erythroid differentiation in MEL cells by repressing the propelling function of wild-type TEL.

It has also been demonstrated that the expression of TEL in Ras-transformed NIH 3T3 cells inhibits cell growth in liquid and soft agar cultures (6). To look at whether the E213/257 mutant modulates the growth of H-Ras-transformed NIH 3T3 cells, we infected these cells with recombinant retroviruses expressing wild-type TEL or the E213/257 mutant. Western analysis confirmed that wild-type TEL and the E213/257 mutant were expressed at similar levels (Fig. 7C). Interestingly, the E213/257 mutant cooperated with Ras to stimulate cell growth in both liquid and semisolid media, while wild-type TEL inhibited growth under both conditions (Fig. 7D and E). All of these data indicate growth-stimulating and transforming activities of the E213/257 mutant in the murine fibroblasts. It is plausible that hyperphosphorylated TEL might act as an inhibitory protein that blocks tumor-suppressive functions of nonhyperphosphorylated TEL.

Extracellular and intracellular signals regulate the phosphorylation status of endogenous TEL. We further analyzed the phosphorylation status of endogenous TEL proteins to clarify a physiological role of their ERK-dependent phosphorylation. We at first induced erythroid differentiation into parental MEL cells by treating them with HMBA. Upon treatment, ERK significantly became dephosphorylated, and thus inactivated, within 8 h, although expression levels of the protein were unchanged (Fig. 8A). In parallel with this result, phosphorylation levels of endogenous TEL proteins were markedly decreased within 1 day. Because hyperphosphorylated TEL blocks erythroid differentiation in MEL cells, dephosphorylation of TEL through the inactivation of ERK could play a role in HMBA-induced differentiation. This finding suggests that ERK could physiologically phosphorylate and thereby inactivate TEL in immature erythroid progenitors to maintain nondifferentiation status.

We next examined phosphorylation levels of endogenous TEL proteins in NIH 3T3 cells. ERK in H-Ras-transformed NIH 3T3 cells was markedly phosphorylated in comparison to that in nontransformed NIH 3T3 cells (Fig. 8B). Notably, the phosphorylation level of endogenous TEL proteins was higher in the former than in the latter. Moreover, the observation that endogenous TEL proteins showed a slight band shift in H-Ras-transformed NIH 3T3 cells supported the increased phosphorylation of TEL by ERK (Fig. 8C). These results indicate that

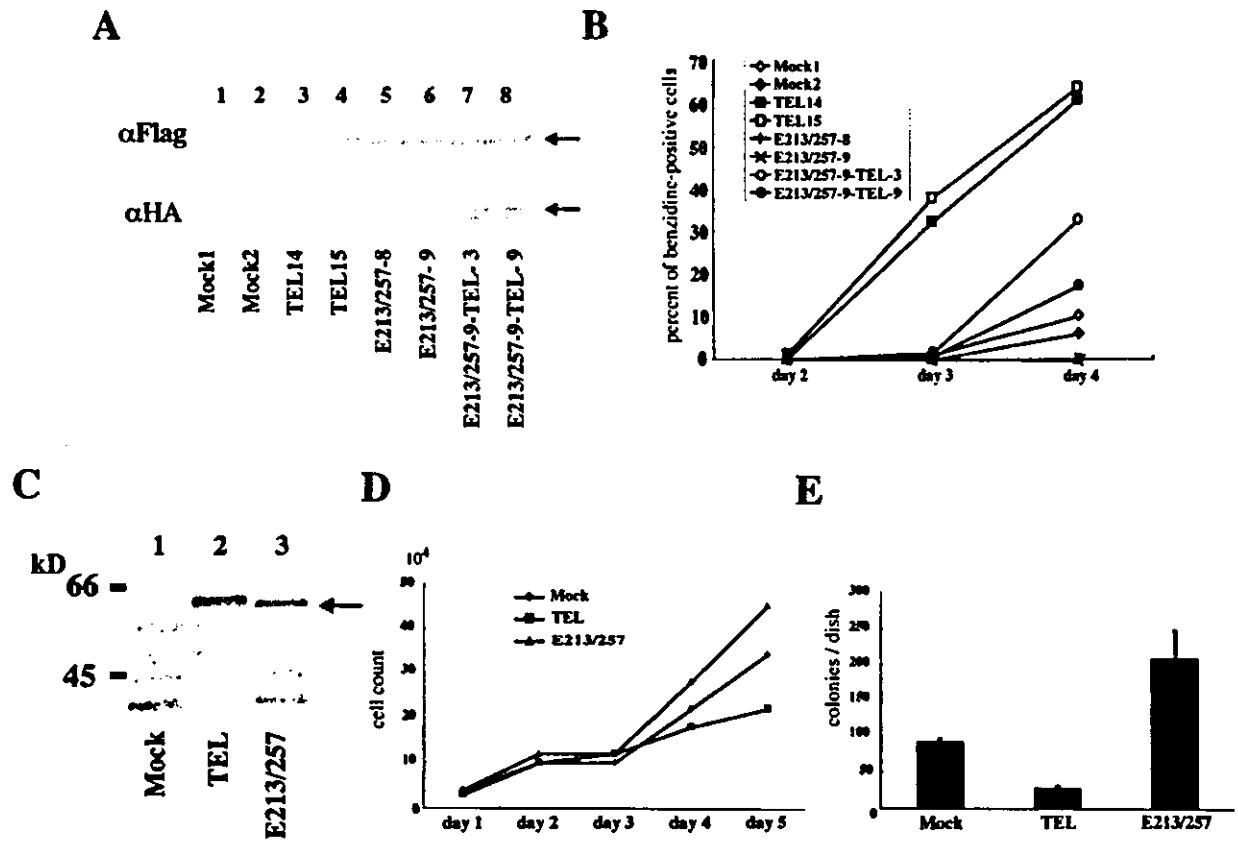

FIG. 7. (A) Expression of wild-type TEL or the E213/257 mutant in MEL clones. These clones were obtained as described in Materials and Methods. Arrows indicate overexpressed wild-type TEL or E213/257 mutant proteins. (B) The E213/257 mutant completely blocked erythroid differentiation in MEL cells after HMBA treatment, and coexpression of wild-type TEL relieved its differentiation block. Cell commitment to terminal differentiation was determined by benzidine staining, and percentages of benzidine-positive cells were calculated at different time points. (C) Expression of wild-type TEL or the E213/257 mutant in H-Ras-transformed NIH 3T3 cells. These H-Ras-transformed NIH 3T3 cells were obtained as described in Materials and Methods. An arrow indicates overexpressed wild-type TEL or E213/257 mutant proteins. (D) The E213/257 mutant stimulates the growth of H-Ras-transformed NIH 3T3 cells in liquid culture. After a total of 2×10^4 cells were plated in 24-well plates, cells were counted every 24 h for 5 days. (E) The E213/257 mutant also stimulates the growth of H-Ras-transformed NIH 3T3 cells in soft agar culture. Transformation assays were performed as described in Materials and Methods. Bars show means and standard deviations of colony counts in two independent experiments that were normalized to colony counts with 2×10^4 NIH 3T3 cells.

Ras/ERK pathways could mediate growth-stimulating signals partly through the inactivation of TEL by phosphorylation.

DISCUSSION

We demonstrated in this study that TEL is hyperphosphorylated in vivo with dependence on ERK activation. Because TEL is efficiently subjected to phosphorylation by ERK in vitro, TEL seems to be a direct target of ERK. According to the results of in vitro kinase assays, both Ser^{213} and Ser^{257} are inducible phosphorylation sites. TEL associates with the CD domain in ERK in vitro, suggesting that the interaction between TEL and ERK may be direct. Importantly, phosphorylation of TEL by overexpressed ERK or endogenous ERK activated by EGF treatment results in the diminishment of its *trans*-repressional effects on the natural EBS promoter. The E213/257 mutant loses its *trans*-repressional activities and functionally mimics hyperphosphorylated TEL, while the corresponding alanine mutant does not lose these activities even through the overexpression of ERK or the activation of endogenous ERK. We conclude that phosphorylation at both Ser^{213} and Ser^{257} is necessary to regulate TEL's molecular functions. Moreover, the glutamate mutant exerts a dominant-negative effect on TEL-mediated transcriptional repression. Therefore, ERK could be a physiologically important MAPK that induces the phosphorylation of TEL and thereby potentially modulates its functions.

Various ETS family transcription factors become phosphorylated by MAPKs and are thereby molecularly activated. The phosphorylating MAP kinases and phosphorylation sites differ among the molecules. TEL is a member of the ETS subfamily with ETS-1 and ETS-2, which possesses a highly conserved N-terminal HLH domain and a C-terminal ETS DNA-binding domain (7). Although the constitutive phosphorylation site Ser^{22} in a TEL molecule is equivalent to Thr^{38} in ETS-1 and Thr^{72} in ETS-2, which are phosphorylated by ERK (38), the ERK-inducible phosphorylation sites Ser^{213} and Ser^{257} are not conserved in ETS1 and ETS2. Moreover, TEL2, a protein that is highly structurally related to TEL (9, 27), also does not possess equivalent serine or threonine residues. Therefore,

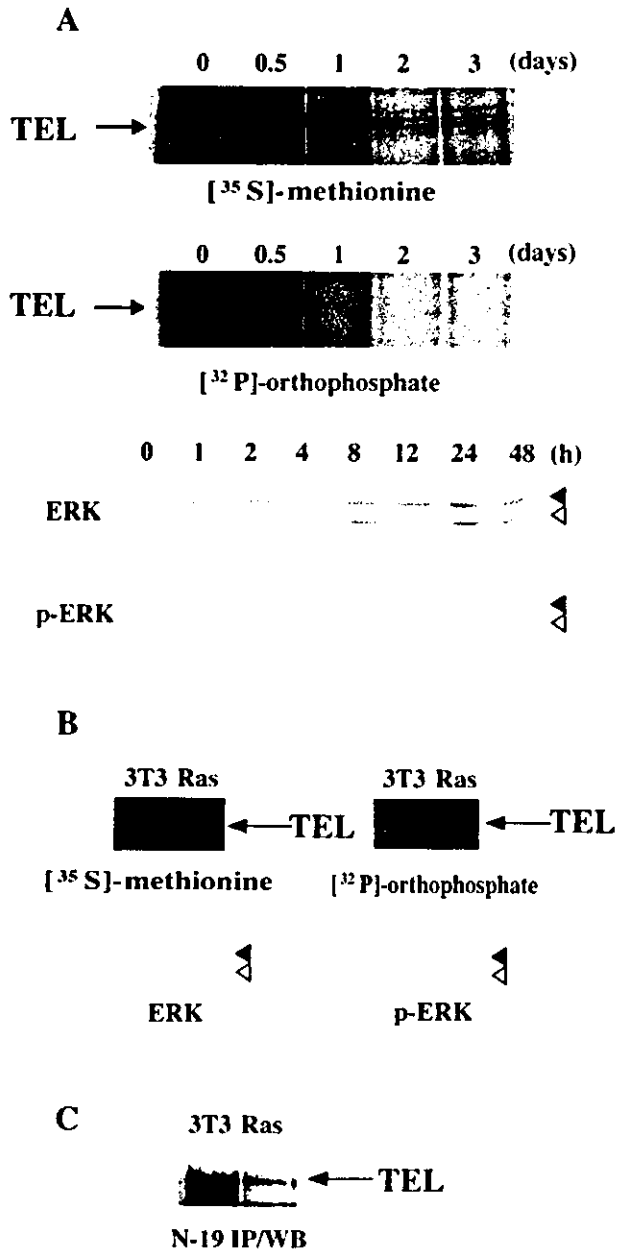

FIG. 8. (A) Dephosphorylation of endogenous TEL proteins during the course of erythroid differentiation in MEL cells. Parental MEL cells were induced into erythroid differentiation with 5 mM HMBA and subjected to metabolic labeling as described in the legend to Fig. 1C (top panel). Western analyses were performed with anti-ERK or anti-phosphorylated ERK antibody to detect total or phosphorylated ERK proteins (bottom panel). Arrows, solid arrowheads, and open arrowheads indicate endogenous TEL, ERK1, and ERK2 proteins, respectively. (B) Phosphorylation of endogenous TEL proteins through Ras/ERK pathways. Nontransformed or H-Ras-transformed NIH 3T3 clones were subjected to metabolic labeling as described for panel A (top panel). Western analyses were performed with anti-ERK or anti-phosphorylated ERK antibody to detect total or phosphorylated ERK proteins (bottom panel). Arrows, solid arrowheads, and open arrowheads indicate endogenous TEL, ERK1, and ERK2 proteins, respectively. (C) Western analysis with anti-TEL antibody (N-19) for immunoprecipitates with the same antibody from mock or H-Ras-transformed NIH 3T3 cells. An arrow indicates immunoprecipitated TEL.

TEL's regulation through ERK-induced phosphorylation appears to be highly characteristic of TEL in the subclass of the ETS transcription factors. Recently, we have reported that TEL also becomes phosphorylated at Ser^{257} by p38 but not by c-Jun NH_2-terminal kinase (1). Although it remains undetermined whether Ser^{213} is also phosphorylated by p38, phosphorylation by both ERK and p38 on the same serine residue in the internal domain is also a unique property of TEL. Both Ras and stress signaling pathways could converge on a transcription factor TEL in the nucleus under certain circumstances.

It has been reported that ERK physically associates with several transcription factors that it phosphorylates, including Elk-1, c-Myc, c-Jun, c-Fos, and AML1 (30). MAPK family members have a CD domain that lies just C terminal to the protein kinase catalytic core within a C-terminal extension shared by the MAPK family and binds to the D domains of substrates outside the phosphoacceptor site (14, 25). Acidic residues in the CD domain of MAPKs are thought to interact with a basic cluster in the D domains of their substrates. This docking reaction facilitates the phosphorylation of substrate phosphoacceptors by MAPK catalytic units by enhancing specificity between a substrate and a relevant MAP kinase. We have demonstrated a physical association between TEL and ERK depending on the CD domain in ERK. This finding may indicate that their interaction is direct. Because TEL is located in the nucleus, ERK that is activated and moves to the nucleus conceivably interacts with TEL. We could not find perfectly matched consensus sequences of the D domain, (R/K)X(R/K)X_{2-4}(L/I)X(L/I), around Ser^{213} and Ser^{257}. Further investigation should be carried out to identify an ERK-binding site in a TEL molecule. Alternatively, it is also possible that ERK indirectly associates with TEL and that unknown factors mediate the association.

Certain transcription factors, including members of the Forkhead family, are negatively regulated through phosphorylation, although its mechanisms are diverse (2, 15). Among the ETS family transcription factors, ETS-2 repressor factor, which exhibits strong transcriptional repressor activity on EBS promoters, becomes phosphorylated by ERK2 and cdc2/cyclin B kinase and loses its suppressive effects through export to the cytoplasm (20). TEL is like EBS-2 repressor factor in that phosphorylation by ERK causes a decrease in *trans*-repressional effects. We investigated possible mechanisms in the prevention of TEL's molecular functions through phosphorylation by using the glutamate mutant that contains substituted glutamates on both Ser^{213} and Ser^{257} and functionally mimics hyperphosphorylated TEL. It is conceivable that a loss of DNA binding to the EBS plays a fundamental role in interfering with transcriptional functions in hyperphosphorylated TEL. Although the identified phosphorylation sites reside outside the ETS DNA-binding domain, the ternary structure of the ETS domain might be changed through the phosphorylation. It is of note that hyperphosphorylated TEL works as a dominant-negative molecule over nonhyperphosphorylated TEL. Considering that the E213/257 mutant described above associates with nonhyperphosphorylated TEL, TEL could lose its transcriptional functions through interaction with a hyperphosphorylated form that does not bind to DNA.

MAPKs are important signal-transducing enzymes that are involved in cell survival regulation and adaptation upon chem-

ical and physical stresses. By and large, ERK and stress MAPKs such as p38 and c-Jun NH_2-terminal kinase mediate opposite signals for cell differentiation and proliferation (25). The activation of ERK is linked to cell survival, whereas that of stress kinases is related to apoptosis induction. We observed that endogenous TEL proteins in NIH 3T3 cells were phosphorylated by endogenous ERK activated through Ras signaling pathways. Moreover, the glutamate mutant mimicking hyperphosphorylated TEL stimulated the growth of Ras-transformed NIH 3T3 cells in liquid and soft agar cultures, in contrast to results obtained with wild-type TEL. Therefore, we conclude that activated ERK represses TEL's inhibitory effects on the natural EBS promoter and thus causes a loss of its tumor-suppressive functions. Because Ras/ERK pathways mediate growth-stimulating signals, this functional regulation of TEL is suitable for ERK's biological roles. On the other hand, some papers suggest that down-regulation of the Ras/ERK signaling pathway is essential for erythroid differentiation in various systems (23, 24, 37). We also showed that ERK was dephosphorylated and thus inactivated during the course of erythroid differentiation with HMBA in MEL cells. In parallel to this phenomenon, endogenous TEL proteins were found to be dephosphorylated upon HMBA treatment. Moreover, the glutamate mutant blocked erythroid differentiation in MEL cells, while wild-type TEL accelerated it. Therefore, the erythroid differentiation stimulator TEL appears to be positively regulated during differentiation through the functional loss of ERK and to play a role in the maturation of erythroid progenitors. All of these data indicate the physiological relevance of the ERK-mediated TEL's phosphorylation. In contrast, the functional significance of the p38-induced phosphorylation in physiological settings remains to be established.

In summary, ERK-induced TEL's phosphorylation results in a loss of its tumor-suppressive functions. Therefore, the functional inactivation of TEL through phosphorylation could be one step in the development and progression of human leukemias. Further studies of the functional regulation of leukemia-related transcription factors will provide some important clues to understanding complex mechanisms in leukemogenesis that have not yet been fully elucidated.

ACKNOWLEDGMENTS

TEL10/pCDNA3, pGL2-754TR, and pCMVMK were generous gifts from T. R. Golub (Dana-Farber Cancer Institute, Boston, Mass.), L. M. Matrisian (Vanderbilt Cancer Center, Nashville, Tenn.), and T. Kadowaki (University of Tokyo, Tokyo, Japan), respectively. pCXN2 and pCAGIPuro were kindly provided by J. Miyazaki (University of Osaka, Osaka, Japan). We thank Y. Furuta for special technical assistance.

This work was financially supported in part by grants-in-aid from the Japan Ministries of both Education, Culture, Sports, Science and Technology and Health, Labor and Welfare and from the Japanese Society for the Promotion of Science. This work was also supported by the Uehara Memorial Foundation and the Japan Intractable Diseases Research Foundation.

REFERENCES

1. **Arai, H., K. Maki, K. Waga, K. Sasaki, Y. Nakamura, Y. Imai, M. Kurokawa, H. Hirai, and K. Mitani.** 2002. Functional regulation of TEL by p38-induced phosphorylation. Biochem. Biophys. Res. Commun. **299**:116–125.
2. **Brunet, A., A. Bonni, M. J. Zigmond, M. Z. Lin, P. Juo, L. S. Hu, M. J. Anderson, K. C. Arden, J. Blenis, and M. E. Greenberg.** 1999. Akt promotes cell survival by phosphorylating and inhibiting a forkhead transcription factor. Cell **96**:857–868.
3. **Buijs, A., L. van Rompaey, A. C. Molijn, J. N. Davis, A. C. O. Vertegaal, M. D. Potter, C. Adams, S. van Baal, E. C. Zwarthoff, M. F. Roussel, and G. C. Grosveld.** 2000. The MN1-TEL fusion protein, encoded by the translocation (12;22)(p13;q11) in myeloid leukemia, is a transcription factor with transforming activity. Mol. Cell. Biol. **20**:9281–9293.
4. **Chang, L., and M. Karin.** 2001. Mammalian MAP kinase signalling cascades. Nature **410**:37–40.
5. **Fenrick, R., J. M. Amann, B. Lutterbach, L. Wang, J. J. Westendorf, J. R. Downing, and S. W. Hiebert.** 1999. Both TEL and AML-1 contribute repression domains to the t(12;21) fusion protein. Mol. Cell. Biol. **19**:6566–6574.
6. **Fenrick, R., L. Wang, J. Nip, J. M. Amann, R. J. Rooney, J. Walker-Daniels, H. C. Crawford, D. L. Hulboy, M. S. Kinch, L. M. Matrisian, and S. W. Hiebert.** 2000. TEL, a putative tumor suppressor, modulates cell growth and cell morphology of Ras-transformed cells while repressing the transcription of *stromelysin-1*. Mol. Cell. Biol. **20**:5828–5839.
7. **Golub, T. R., G. F. Barker, M. Lovett, and D. G. Gilliland.** 1994. Fusion of PDGF receptor β to a novel *ets*-like gene, tel, in chronic myelomonocytic leukemia with t(5;12) chromosomal translocation. Cell **77**:307–316.
8. **Golub, T. R., A. Goga, G. F. Barker, D. E. Afar, J. McLaughlin, S. K. Bohlander, J. D. Rowley, O. N. Witte, and D. G. Gilliland.** 1996. Oligomerization of the ABL tyrosine kinase by the Ets protein. Mol. Cell. Biol. **16**:4107–4116.
9. **Gu, X., B. H. Shin, Y. Akbarali, A. Weiss, J. Boltax, P. Oettgen, and T. A. Libermann.** 2001. Tel-2 is a novel transcriptional repressor related to the Ets factor Tel/ETV-6. J. Biol. Chem. **276**:9421–9436.
10. **Guidez, F., K. Petrie, A. M. Ford, H. Lu, C. A. Bennett, A. MacGregor, J. Hannemann, Y. Ito, J. Ghysdael, M. Greaves, L. M. Wiedemann, and A. Zelent.** 2000. Recruitment of the nuclear receptor corepressor N-CoR by the TEL moiety of the childhood leukemia-associated TEL-AML1 oncoprotein. Blood **96**:2557–2561.
11. **Hiebert, S. W., W. Sun, J. N. Davis, T. Golub, S. Shurtleff, A. Buijs, J. Downing, G. Grosveld, M. F. Roussel, D. G. Gilliland, N. Lenny, and S. Meyers.** 1996. The t(12;21) translocation converts AML-1B from an activator to a repressor of transcription. Mol. Cell. Biol. **16**:1349–1355.
12. **Jousset, C., C. Carron, A. Boureux, C. T. Quang, C. Oury, I. Dusanter-Fourt, M. Charon, J. Levin, O. Bernard, and J. Ghysdael.** 1997. A domain of TEL conserved in a subset of ETS proteins defines a specific oligomerization interface essential to the mitogenic properties of the TEL-PDGFRβ oncoprotein. EMBO J. **16**:69–82.
13. **Kim, C. A., M. L. Phillips, W. Kim, M. Gingery, H. H. Tran, M. A. Robinson, S. Faham, and J. U. Bowie.** 2001. Polymerization of the SAM domain of TEL in leukemogenesis and transcriptional repression. EMBO J. **20**:4173–4182.
14. **Kolch, W.** 2000. Meaningful relationship: the regulation of the Ras/Raf/MEK/ERK pathways by protein interactions. Biochem. J. **351**:289–305.
15. **Kops, G. J. P. L., N. D. de Ruiter, A. M. M. de Vries-Smits, D. R. Powell, J. L. Bos, and B. M. T. Burgering.** 1999. Direct control of the Forkhead transcription factor AFX by protein kinase B. Nature **398**:630–634.
16. **Kuno, Y., A. Abe, N. Emi, M. Iida, T. Yokozawa, M. Towatari, M. Tanimoto, and H. Saito.** 2001. Constitutive kinase activation of the *TEL-Syk* fusion gene in myelodysplastic syndrome with t(9;12)(q22;p13). Blood **97**:1050–1055.
17. **Kurokawa, M., K. Mitani, T. Yamagata, T. Tanaka, K. Izutsu, S. Ogawa, T. Moriguchi, E. Nishida, Y. Yazaki, and H. Hirai.** 2000. The Evi-1 oncoprotein inhibits c-Jun N-terminal kinase and prevents stress-induced cell death. EMBO J. **19**:2958–2968.
18. **Kwiatkowski, B. A., L. S. Bastian, T. R. Bauer, Jr., S. Tsai, A. G. Zielinska-Kwiatkowska, and D. D. Hickstein.** 1998. The *ets* family member Tel binds to the Fli-1 oncoprotein and inhibits its transcriptional activity. J. Biol. Chem. **273**:17525–17530.
19. **Lacronique, V., A. Boureux, V. D. Valle, H. Poirel, C. T. Quang, M. Mauchauffe, C. Berthou, M. Lessard, R. Berger, J. Ghysdael, and O. A. Bernard.** 1997. A TEL-JAK2 fusion protein with constitutive kinase activity in human leukemia. Science **278**:1309–1312.
20. **Le Gallic, L., D. Sgouras, G. Beal, Jr., and G. Mavrothalassitis.** 1999. Transcriptional repressor ERF is a Ras/mitogen-activated protein kinase target that regulates cellular proliferation. Mol. Cell. Biol. **19**:4121–4133.
21. **Lopez, R. G., C. Carron, C. Oury, P. Gardellin, O. Bernard, and J. Ghysdael.** 1999. TEL is a sequence-specific transcriptional repressor. J. Biol. Chem. **274**:30132–30138.
22. **Maki, K., K. Mitani, T. Yamagata, M. Kurokawa, Y. Kanda, Y. Yazaki, and H. Hirai.** 1999. Transcriptional inhibition of p53 by MLL/MEN chimeric protein found in myeloid leukemia. Blood **93**:3216–3224.
23. **Matsuzaki, T., K. Aisaki, Y. Yamamura, M. Noda, and Y. Ikawa.** 2000. Induction of erythroid differentiation by inhibition of Ras/ERK pathway in a Friend murine leukemia cell line. Oncogene **19**:1500–1508.
24. **Miyazaki, R., H. Ogata, and Y. Kobayashi.** 2001. Requirement of thrombopoietin-induced activation of ERK for megakaryocyte differentiation and of p38 for erythroid differentiation. Ann. Hematol. **80**:284–291.
25. **Pearson, G., F. Robinson, T. B. Gibson, B. E. Xu, M. Karandikar, K. Berman, and M. H. Cobb.** 2001. Mitogen-activated protein (MAP) kinase pathways: regulation and physiological functions. Endocr. Rev. **22**:153–183.
26. **Poirel, H., C. Oury, C. Carron, E. Duprez, Y. Laabi, A. Tsapis, S. P. Romana, M. Mauchauffe, M. Le Coniat, R. Berger, J. Ghysdael, and O. A. Bernard.**

1997. The TEL gene products: nuclear phosphoproteins with DNA binding properties. Oncogene **14**:349–357.

27. **Potter, M. D., A. Buijs, B. Kreider, L. van Rompaey, and G. Grosveld.** 2000. Identification and characterization of a new human ETS-family transcription factor, TEL2, that is expressed in hematopoietic tissues and can associate with *TEL1/ETV6*. Blood **95**:3341–3348.
28. **Rabault, B., M. F. Roussel, C. T. Quang, and J. Ghysdael.** 1996. Phosphorylation of Ets1 regulates the complementation of a CSF-1 receptor impaired in mitogenesis. Oncogene **13**:877–881.
29. **Slupsky, C. M., L. N. Gentile, L. W. Donaldson, C. D. Mackereth, J. J. Seidel, B. J. Graves, and L. P. McIntosh.** 1998. Structure of the Ets-1 pointed domain and mitogen-activated protein kinase phosphorylation site. Proc. Natl. Acad. Sci. USA **95**:12129–12134.
30. **Tanaka, T., M. Kurokawa, K. Ueki, K. Tanaka, Y. Imai, K. Mitani, K. Okazaki, N. Sagata, Y. Yazaki, Y. Shibata, T. Kadowaki, and H. Hirai.** 1996. The extracellular signal-regulated kinase pathway phosphorylates AML1, an acute myeloid leukemia gene product, and potentially regulates its transactivation ability. Mol. Cell. Biol. **16**:3967–3979.
31. **Ueki, K., S. Matsuda, K. Tobe, Y. Gotoh, H. Tamemoto, M. Yachi, Y. Akanuma, Y. Yazaki, E. Nishida, and T. Kadowaki.** 1994. Feedback regulation of mitogen-activated protein kinase kinase activity of c-Raf-1 by insulin and phorbol ester stimulation. J. Biol. Chem. **269**:15756–15761.
32. **Van Rompaey, L., M. Potter, C. Adams, and G. Grosveld.** 2000. Tel induces a G1 arrest and suppresses Ras-induced transformation. Oncogene **19**:5244–5250.
33. **Waga, K., Y. Nakamura, K. Maki, H. Arai, T. Yamagata, K. Sasaki, M. Kurokawa, H. Hirai, and K. Mitani.** 2003. Leukemia-related transcription factor TEL accelerates differentiation of Friend erythroleukemia cells. Oncogene **22**:59–68.
34. **Wang, L., and S. W. Hiebert.** 2001. TEL contacts multiple co-repressors and specifically associates with histone deacetylase-3. Oncogene **20**:3716–3725.
35. **Wang, L. C., F. Kuo, Y. Fujiwara, D. G. Gilliland, T. R. Golub, and S. H. Orkin.** 1997. Yolk sac angiogenesis defect and intra-embryonic apoptosis in mice lacking the Ets-related factor TEL. EMBO J. **16**:4374–4383.
36. **Wang, L. C., W. Swat, Y. Fujiwara, L. Davidson, J. Visvader, F. Kuo, F. W. Alt, D. G. Gilliland, T. R. Golub, and S. H. Orkin.** 1998. The *TEL/ETV6* gene is required specifically for hematopoiesis in the bone marrow. Genes Dev. **12**:2392–2402.
37. **Witt, O., K. Sand, and A. Pekrun.** 2000. Butyrate-induced erythroid differentiation of human K562 leukemia cells involves inhibition of ERK and activation of p38 MAP kinase pathways. Blood **95**:2391–2396.
38. **Yang, B. S., C. A. Hauser, G. Henkel, M. S. Colman, C. van Beveren, K. J. Stacey, D. A. Hume, R. A. Maki, and M. C. Ostrowski.** 1996. Ras-mediated phosphorylation of a conserved threonine residue enhances the transactivation activities of c-Ets1 and c-Ets2. Mol. Cell. Biol. **16**:538–547.
39. **Yang, S. H., A. Galanis, and A. D. Sharrocks.** 1999. Targeting of p38 mitogen-activated protein kinases to MEF2 transcription factors. Mol. Cell. Biol. **19**:4028–4038.

MOLECULAR AND CELLULAR BIOLOGY, Feb. 2004, p. 1033–1043 Vol. 24, No. 3
0270-7306/04/$08.00+0 DOI: 10.1128/MCB.24.3.1033–1043.2004

The Corepressor mSin3A Regulates Phosphorylation-Induced Activation, Intranuclear Location, and Stability of AML1

Yoichi Imai,[1] Mineo Kurokawa,[1]* Yuko Yamaguchi,[1] Koji Izutsu,[1] Eriko Nitta,[1] Kinuko Mitani,[2] Masanobu Satake,[3] Tetsuo Noda,[4] Yoshiaki Ito,[5] and Hisamaru Hirai[1]

Department of Hematology and Oncology, Graduate School of Medicine, University of Tokyo, Bunkyo-ku, Tokyo 113-8655,[1] Department of Hematology, Dokkyo University School of Medicine, Tochigi 321-0207,[2] Department of Molecular Immunology, Institute of Development, Aging, and Cancer, Tohoku University, Sendai 980-0872,[3] and Department of Cell Biology, The Cancer Institute, Japanese Foundation for Cancer Research, Tokyo 170-0012,[4] Japan, and Institute of Molecular and Cell Biology, National University of Singapore, Singapore 117609, Singapore[5]

Received 17 March 2003/Returned for modification 8 May 2003/Accepted 31 October 2003

The *AML1* (*RUNX1*) gene, one of the most frequent targets of translocations associated with human leukemias, encodes a DNA-binding protein that plays pivotal roles in myeloid differentiation through transcriptional regulation of various genes. Previously, we reported that AML1 is phosphorylated on two serine residues with dependence on activation of extracellular signal-regulated kinase, which positively regulates the transcriptional activity of AML1. Here, we demonstrate that the interaction between AML1 and the corepressor mSin3A is regulated by phosphorylation of AML1 and that release of AML1 from mSin3A induced by phosphorylation activates its transcriptional activity. Furthermore, phosphorylation of AML1 regulates its intranuclear location and disrupts colocalization of AML1 with mSin3A in the nuclear matrix. PEBP2β/CBFβ, a heterodimeric partner of AML1, was shown to play a role in protecting AML1 from proteasome-mediated degradation. We show that mSin3A also protects AML1 from proteasome-mediated degradation and that phosphorylation-induced release of AML1 from mSin3A results in degradation of AML1 in a time-dependent manner. This study provides a novel regulatory mechanism for the function of transcription factors mediated by protein modification and interaction with cofactors.

AML1 (*RUNX1*) was first identified on chromosome 21 as the gene that is disrupted in the (8;21)(q22;q22) translocation, which is one of the most frequent chromosome abnormalities associated with acute myelogenous leukemia (AML) (20, 24, 29). *AML1* is also disrupted in t(3;21)(q26;q22), which is found in the blastic crisis phase of chronic myelogenous leukemia (23). It was also reported that the *AML1* gene is rearranged in acute lymphoblastic leukemia carrying t(12;21)(p12;q22) and that this translocation generates the TEL-AML1 fusion protein (5, 34). Furthermore, point mutations in the Runt domain of the *AML1* gene were found in patients with AML (31, 33), familial platelet disorder with predisposition to AML (35), or myelodysplastic syndrome (9). These findings suggest that the structural alterations of AML1 caused by translocations or point mutations trigger leukemic transformation of hematopoietic cells.

AML1 regulates the transcription of various genes that are important in hematopoiesis (27, 36, 37, 48). Furthermore, it has been revealed that AML1 can cause neoplastic transformation when overexpressed in fibroblasts, suggesting a potential role for AML1 in promoting cellular proliferation (17). From analyses of mice lacking *AML1*, it was shown that AML1 plays an important role in liver-derived hematopoiesis and angiogenesis (30, 38).

Previously, the regulatory mode of AML1 functions through signal transduction pathways was investigated, and it was revealed that AML1 is phosphorylated with dependence on the activation of extracellular signal-regulated kinase (ERK) (40). ERK-dependent phosphorylation enhances the transcriptional activity of AML1, and mutations of the phosphorylation sites reduce the transforming capacity of AML1 in fibroblasts (40). These results indicate that the functions of AML1 are potentially regulated by ERK-induced phosphorylation, which is activated by cytokine and growth factor stimuli. However, the mechanism by which the transcriptional ability of AML1 is activated by phosphorylation has not been clear.

A growing number of proteins have been shown to interact with AML1 to modify its function (2, 10, 12, 19, 21, 28, 44). Here, we have investigated whether these protein-protein interactions are affected by phosphorylation of AML1, and we found that the corepressor mSin3A is released from phosphorylated AML1, whereby the transcriptional activity of phosphorylated AML1 is activated. Furthermore, we demonstrated that mSin3A is a key regulator for the intranuclear localization and stability of AML1. This study reveals a previously unappreciated role of the corepressor mSin3A as a regulator of AML1.

MATERIALS AND METHODS

Plasmid construction. The pME-AML1, pME-PEBP2β, pCMV-MK, and Tww-tk-Luc reporter plasmids were constructed as described previously (41). The AML1 mutants S249/266A and S249/266E were obtained by replacing the serine residues with alanines or glutamic acids by the site-directed mutagenesis method for AML1 cDNA (15). FLAG-tagged AML1 constructs were generated as described previously (10). The deletion mutant of S249/266A, Δ(181-210)SA,

* Corresponding author. Mailing address: Department of Hematology and Oncology, Graduate School of Medicine, University of Tokyo, 7-3-1 Hongo, Bunkyo-ku, Tokyo 113-8655, Japan. Phone: 81-3-38150-5411, ext. 33118. Fax: 81-3-3815-8350. E-mail: kurokawa-tky@umin.ac.jp.

was created by PCR from S249/266A with the insertion of a *Bgl*II site to join the fragments. The carboxy-terminal deletion mutant, AML1 1-288, was generated as described previously (17).

Cell culture and DNA transfection. COS-7 cells were grown in Dulbecco's modified Eagle's medium (DMEM) supplemented with 10% fetal calf serum (FCS). HEL cells were cultured in RPMI 1640 supplemented with 10% FCS. P19 mouse embryonal carcinoma cells were cultured as described previously (40). COS-7 and P19 cells were transfected with expression plasmids using SuperFect Transfection Reagent (Qiagen Inc.). Mouse embryonic fibroblasts from normal and PEBP2β-deficient mice (26) were transfected with expression plasmids by using Effectene Transfection Reagent (Qiagen Inc.).

Immunoprecipitation and Western blotting. COS-7 cells were cultured for 30 to 35 h after transfection in DMEM containing 10% FCS and then transferred to DMEM containing 0.1% FCS and incubated for 12 to 15 h. They were then either not treated or treated for 5 min with 10% FCS plus 100 ng of recombinant human epidermal growth factor (EGF) (Sigma) per ml and harvested in phosphate-buffered saline supplemented with 1 mM EDTA, 1.5 mg of iodoacetamide/ml, 0.2 mM phenylmethylsulfonyl fluoride, 0.1 trypsin inhibitory unit/ml of aprotinin, 25 mM β-glycerophosphate, and 0.5% Triton X-100. These cell lysates were precleared with protein G-Sepharose (Pharmacia), mixed with the anti-mSin3A antibody K-20 (Santa Cruz), and rotated for 2 h; this was followed by recovery of mSin3A on protein G-Sepharose beads. The beads were washed four times with the lysis buffer. Immunoprecipitates were subjected to sodium dodecyl sulfate-polyacrylamide gel electrophoresis (SDS-PAGE) and Western blotting with the anti-FLAG M2 monoclonal antibody (Sigma).

HEL cells (10^7) were harvested in 1% Triton lysis buffer (10 mM Tris-HCl, pH 7.4, 5 mM EDTA, 150 mM NaCl, 1% Triton-X, 10% glycerol, 10 U of aprotinin/ml, 2 mM phenylmethylsulfonyl fluoride, 25 mM β-glycerophosphate), and the cell lysates were precleared with protein G-Sepharose. The same amount of cell lysates was mixed with rabbit polyclonal immunoglobulin G (IgG) (Santa Cruz) as a control or with anti-AML1 antibody (Ab-1; Oncogene), and rotated for 12 h; this was followed by recovery of AML1 on protein G-Sepharose beads. The beads were washed four times with the lysis buffer. Immunoprecipitates were subjected to SDS-PAGE and Western blotting with anti-mSin3A antibody.

We lysed the PEBP2β-deficient fibroblasts with 1% Triton lysis buffer, and the cell lysates were subjected to SDS-PAGE and Western blotting with anti-FLAG M2 monoclonal antibody, anti-PEBP2β antibody, or anti-actin monoclonal antibody (Chemicon International). The anti-PEBP2β antibody was prepared as described elsewhere (39). To block proteolysis, lactacystin (10 mM) dissolved in dimethyl sulfoxide was added to the cell culture medium overnight.

Chromatin and nuclear matrix fractions were prepared by sequential extraction with cytoskeleton buffer and digestion buffer followed by 0.25 M ammonium sulfate extraction in a biochemical-fractionation assay as described previously (47). To detect lamin B1 localized in the nuclear matrix, we used anti-lamin B1 antibody (M-20) (Santa Cruz).

Transcriptional-response assays. Luciferase assays were performed as described previously (8). Briefly, reporter and expression plasmids were transfected into P19 or COS-7 cells by a SuperFect protocol. P19 cells were harvested and subjected to the luciferase assay after 30 to 36 h of transfection. COS-7 cells were starved in DMEM containing 0.1% FCS with or without lactacystin, harvested, and subjected to the luciferase assay after 12 h of transfection. The data were normalized using the internal control of transfection efficiency, as described previously (8).

Immunofluorescence and in situ nuclear matrix isolation. COS-7 cells transfected with expression plasmids were fixed in 3.7% formaldehyde in phosphate-buffered saline. They were treated with the anti-FLAG and anti-mSin3A antibodies and then incubated with Texas-red-conjugated donkey anti-mouse IgG and fluorescein isothiocyanate-conjugated donkey anti-rabbit IgG (Jackson Immuno Research Laboratories, Inc.), respectively, as secondary antibodies, as described previously (8, 16). In situ nuclear matrices were prepared as described elsewhere (46, 47).

RESULTS

ERK-mediated phosphorylation disrupts the interaction of AML1 with mSin3A. It has been demonstrated that AML1 is phosphorylated on serines 249 and 266 by ERK and that phosphorylation of AML1 activates the transcriptional activity (40). To elucidate the mechanism for phosphorylation-induced activation of AML1, we analyzed the interaction of AML1 with other proteins when it is phosphorylated.

It has been shown that AML1 associates with the mSin3A corepressor (21). Consistent with these observations, we found that FLAG-tagged AML1 is coimmunoprecipitated with mSin3A by the anti-mSin3A antibody when it is overexpressed together with PEBP2β in COS-7 cells (Fig. 1A, lane 1). When COS-7 cells were cotransfected with FLAG-tagged AML1 and PEBP2β plus ERK and stimulated with EGF, we observed shifted bands of AML1 mirroring its phosphorylation (40) (Fig. 1A, lane 4). Significantly, the amount of AML1 coimmunoprecipitated with mSin3A was markedly reduced upon phosphorylation (Fig. 1A, lane 2). The total amount of AML1 was constant regardless of overexpression of ERK combined with EGF stimulation (Fig. 1A, lanes 3 and 4). These results suggest that AML1 dissociates from mSin3A when it is phosphorylated by ERK.

The previous study showed that glutamic acid mimics the negative charge of phosphate and that some glutamic acid mutants of serine act like a phosphorylated form of the cognate wild-type proteins (11, 22). To confirm that ERK-mediated phosphorylation can abrogate the ability of AML1 to interact with mSin3A, we generated the mutant of AML1 that mimics phosphorylated AML1, in which serines 249 and 266 of AML1 were changed to glutamic acids (S249/266E). SDS-PAGE and Western blotting revealed that S249/266E showed a mobility shift similar to that of phosphorylated AML1 when expressed in COS-7 cells (Fig. 1B, lane 7). As shown in Fig. 1B, we found by using a coimmunoprecipitation assay that S249/266E had completely lost the ability to interact with mSin3A, although wild-type AML1 was readily coimmunoprecipitated with mSin3A. It had already been shown that the mutant in which serines 249 and 266 were changed to alanines (S249/266A) is not phosphorylated even upon ERK activation (40). In contrast to S249/266E, S249/266A was coimmunoprecipitated with mSin3A as efficiently as wild-type AML1 (Fig. 1B, lane 4). In these experiments, the amounts of wild-type AML1, S249/266E, and S249/266A were almost the same when cotransfected with PEBP2β, which is known to protect AML1 from proteolytic degradation (Fig. 1B, lanes 6 to 8). These results suggest that phosphorylation disrupts the ability of AML1 to heterodimerize with mSin3A.

To confirm that AML1 and mSin3A form a complex in hematopoietic cells, we investigated the interactions between endogenous AML1 and mSin3A in HEL cells, a human erythroleukemia-derived cell line. Endogenous mSin3A is not immunoprecipitated by normal rabbit polyclonal IgG in HEL cells (Fig. 1C, lane 1). On the other hand, the precipitate by the anti-AML1 antibody (Ab-1) contains endogenous mSin3A (Fig. 1C, lane 2). In the previous study, the anti-AML1 antibody (Ab-1) was shown to immunoprecipitate endogenous AML1 in HEL cells (21). These results indicate that mSin3A binds to AML1 in hematopoietic cells.

Transcriptional activity of unphosphorylated AML1 is recovered by addition of HDAC inhibitor. In a previous study, it was shown that ERK-dependent phoshphorylation of AML1 can potentiate its transcriptional ability (40). However, the identities of regulatory proteins that repress the transcriptional activity of unphosphorylated AML1 have not been well characterized. Given the interaction between AML1 and mSin3A, it might be that mSin3A plays an important role in the repression of AML1 transcriptional activity. Histone deacetylases

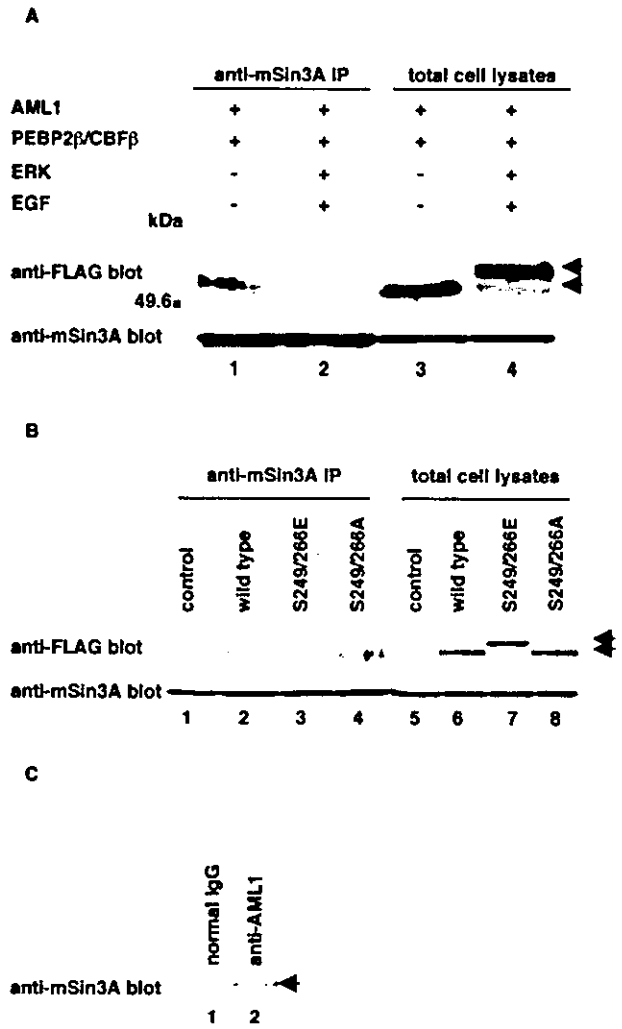

FIG. 1. Analyses of the interaction between phosphorylated AML1 and mSin3A. (A) COS-7 cells were transfected with pME-FLAG-AML1 and pME-PEBP2β, together with pRc/CMV (lanes 1 and 3) or pCMVMK (lanes 2 and 4), starved in medium containing 0.1% FCS, treated for 5 min with 100 ng of EGF per ml plus 10% FCS (lanes 2 and 4) or left untreated (lanes 1 and 3), and harvested with lysis buffer. The cell lysates were precleared with protein G-Sepharose, mixed with anti-mSin3A antibody, and rotated for 2 h at 4°C. Then, mSin3A was recovered on protein G-Sepharose beads. The washed beads were subjected to SDS-PAGE, followed by Western blotting with anti-FLAG or anti-mSin3A antibody. Expression of each protein was monitored by using 60 μg of total cell lysates. +, present; −, absent; IP, immunoprecipitate; arrows, phosphorylated and unphosphorylated AML1. (B) COS-7 cells were transfected with pME18S, pME-FLAG-AML1, pME-FLAG-S249/266E, or S249/266A with pME-PEBP2β and harvested with lysis buffer. The cell lysates were precleared with protein G-Sepharose, mixed with anti-mSin3A antibody, and rotated for 2 h at 4°C. Then, mSin3A was recovered on protein G-Sepharose beads. The washed beads were subjected to SDS-PAGE, followed by Western blotting with the anti-FLAG or anti-mSin3A antibody. Expression of each protein was monitored by using 60 μg of total cell lysates. Arrows indicate wild-type and mutant AML1. (C) HEL cells were harvested with lysis buffer, and the cell lysates were precleared with protein G-Sepharose. The same amount of cell lysates was mixed with anti-AML1 antibody (Ab-1) or rabbit polyclonal IgG and rotated for 12 h; this was followed by recovery of AML1 on protein G-Sepharose beads. The washed beads were subjected to SDS-PAGE and Western blotting with anti-mSin3A antibody. Arrow, AML1.

(HDACs) that are recruited by mSin3A mediate transcriptional repression by rendering the nearby chromatin inaccessible to transcriptional activators through deacetylation of histone proteins (32, 42). Trichostatin A (TSA), a specific HDAC inhibitor, has been shown to relieve transcriptional repression by AML1, suggesting a role for mSin3A-HDAC in the repressor activity of AML1 (21). Therefore, we investigated whether unphosphorylated AML1 can be derepressed when mSin3A-HDAC is inhibited by TSA in a transcriptional-response assay.

When AML1 and ERK were cotransfected into P19 cells with the Tww-tk-Luc reporter that can be activated by AML1, we observed a fivefold induction of transcriptional activity compared to overexpression of ERK alone (Fig. 2A, lane 2). On the other hand, when S249/266A was coexpressed with ERK, only 1.5-fold induction of the transcriptional activity was observed (Fig. 2A, lane 3), which is consistent with our previous report. Upon treatment with TSA, both wild-type AML1 and S249/266A cotransfected with ERK induced 2.5-fold transcriptional activity compared to overexpression of ERK alone, and the reduced transcriptional activity of S249/266A in the absence of TSA was restored to a level similar to that of wild-type AML1 (Fig. 2B, lanes 2 and 3). These results suggest that the transcriptional activity of unphosphorylated AML1 is suppressed by the interaction with mSin3A-HDAC.

Intranuclear targeting of AML1 is induced by its phosphorylation. The previous study showed that AML1 is localized in the nuclear matrix, a subnuclear organization, and that a nuclear-matrix-targeting sequence has been identified within its carboxyl-terminal domain (47). Furthermore, it was shown that mSin3A is also located in the nuclear matrix, accompanied by HDACs, and represses transcription there (43). Given that the physical interaction between AML1 and mSin3A is disrupted by phosphorylation of AML1, we investigated whether targeting of AML1 to the nuclear matrix could be affected upon phosphorylation.

FLAG-tagged AML1, PEBP2β, and ERK were coexpressed in COS-7 cells, and the cells were cultured with or without EGF. They were stained with the anti-FLAG and anti-mSin3A antibodies. Both AML1 and endogenous mSin3A were localized predominantly in the nucleus regardless of EGF stimulation (data not shown). The AML1 mutants, S249/266A and S249/266E, are also located in the nucleus (data not shown). Next, we analyzed the cells in in situ nuclear-matrix preparations (46, 47). Staining the nuclear matrix with anti-FLAG and anti-mSin3A antibodies revealed that AML1 and mSin3A were colocalized in the nuclear matrix without EGF stimulation (Fig. 3A to C). When we stimulated the transfected cells with EGF, mSin3A was detected in the nuclear matrix (Fig. 3E). Under these conditions, however, AML1 was absent from the nuclear matrix, where no colocalization signal of AML1 and mSin3A was detected (Fig. 3D and F). Subsequently, we investigated the intranuclear localization of S249/266A and S249/266E. As shown in Fig. 3, S249/266A and mSin3A were colocalized in the nuclear matrix (Fig. 3G to I), whereas S249/266E was neither detected in the nuclear matrix nor colocalized with mSin3A (Fig. 3J to L). These results indicate that AML1 and mSin3A are colocalized in the nuclear matrix when AML1 is not phosphorylated and that AML1 translocates from the nuclear matrix upon phosphorylation.

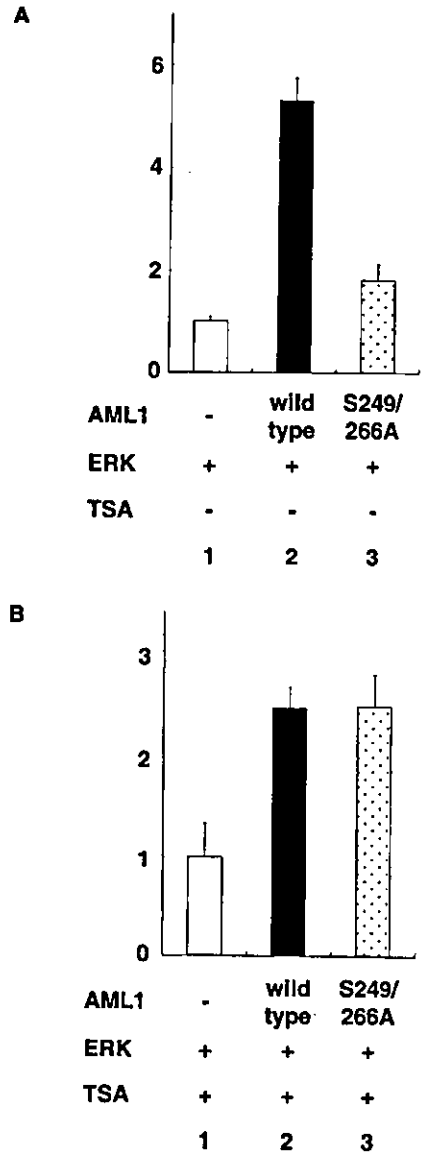

FIG. 2. Transcriptional response assays of AML1 and its unphosphorylated mutant in the presence of TSA. P19 cells were cotransfected with 500 ng of Tww-tk-Luc, 200 ng of pCMVMK, and 20 ng of pME18S AML1, −), pME-AML1 (AML1, wild type), or pME-S249/266A as indicated with (B) or without (A) treatment with TSA. The cells were cultured for 30 to 36 h after transfection and harvested. The means and standard deviations of the luciferase activities of AML1 and S249/266A in two independent transfections are shown. We used the mean of the luciferase activities of the expression vector (pME18S) in two independent transfections as the control. Similar results were obtained in four additional independent transfections.

A specific domain that interacts with mSin3A has been mapped to residues 181 to 210 within AML1 (21). To manifest a correlation between mSin3A binding and nuclear localization of AML1, we tested the intranuclear distribution of the AML1 deletion mutant that lacks the domain interacting with mSin3A. To rule out the possibility of phosphorylation-induced release of mSin3A from the mutant, we changed serines 249 and 266 to alanines in AML1Δ(181-210), which generates the double mutant, Δ(181-210)SA. We introduced FLAG-tagged Δ(181-210)SA, together with PEBP2β, into COS-7 cells and assessed the interaction with mSin3A by a coimmunoprecipitation assay. The expression levels of wild-type AML1 and Δ(181-210)SA were almost the same when they were overexpressed with PEBP2β (Fig. 4A, lanes 5 and 6). Consistent with the previous report, Δ(181-210)SA was hardly coimmunoprecipitated with mSin3A by the anti-mSin3A antibody, in contrast to wild-type AML1 (Fig. 4A, lanes 2 and 3). Next, we confirmed the intranuclear localization of Δ(181-210)SA. FLAG-tagged wild-type AML1 or Δ(181-210) SA was introduced into COS-7 cells, and the cells were stained with the anti-FLAG and anti-mSin3A antibodies. Both forms of AML1 were visualized exclusively in the nucleus by whole-cell staining (Fig. 4B and E). Wild-type AML1 was consistently colocalized with mSin3A, whereas Δ(181-210)SA showed altered nuclear distribution, which does not coincide with that of mSin3A (Fig. 4D and G). In in situ nuclear matrix preparations, wild-type AML1 and mSin3A were colocalized in the nuclear matrix (Fig. 4H to J). In contrast, Δ(181-210)SA was not detected in the nuclear matrix, where mSin3A was invariably located (Fig. 4K to M). The data we obtained indicate that targeting of AML1 to the nuclear matrix is dependent on the interaction with mSin3A, which suggests that AML1 is tethered to the nuclear matrix by mSin3A. These results are consistent with our findings that phosphorylation-induced release from mSin3A translocates AML1 from the nuclear matrix.

To substantiate our finding that the intranuclear targeting of AML1 is induced by its phosphorylation, we performed a biochemical-fractionation assay (Fig. 5). Wild-type AML1 and S249/266A are detected in the fractions of chromatin and the nuclear matrix, whereas S249/266E is present exclusively in the chromatin fraction. These findings are consistent with the results showing that AML1 translocates from the nuclear matrix upon phosphorylation in in situ immunofluorescence analyses. Furthermore, Δ(181-210)SA is also undetectable in the nuclear-matrix fraction, again suggesting the requirement for mSin3A interaction in nuclear-matrix targeting of AML1

Next, we investigated whether a mutation in the nuclear-matrix attachment site of AML1 affects interaction with mSin3A. It was shown that the carboxy terminus of AML1 contains a segment essential for association with the nuclear matrix (47). Therefore, we generated a carboxy-terminal deletion mutant, AML1 1-288, and overexpressed it in COS-7 cells. In biochemical-fractionation assays, AML1 1-288 is shown to be released from the nuclear matrix (Fig. 5, lane 10). As shown in Fig. 6, AML1 1-288 has lost the ability to interact with mSin3A. These results suggest that the nuclear sublocalization of AML1 plays an important role in interaction with mSin3A.

Stability of phosphorylated AML1 proteins in COS-7 cells. AML1 is continuously subjected to proteolytic degradation mediated by the ubiquitin-proteasome pathway, which is blocked by heterodimerization with PEBP2β (7). mSin3A is also known to block proteasome-mediated degradation of proteins, such as p53 (49). Given the phosphorylation-dependent interaction of AML1 with mSin3A, we examined the stability of phosphorylated AML1 to elucidate a potential role of mSin3A in proteasome-mediated degradation of AML1. COS-7 cells were transfected with FLAG-tagged wild-type

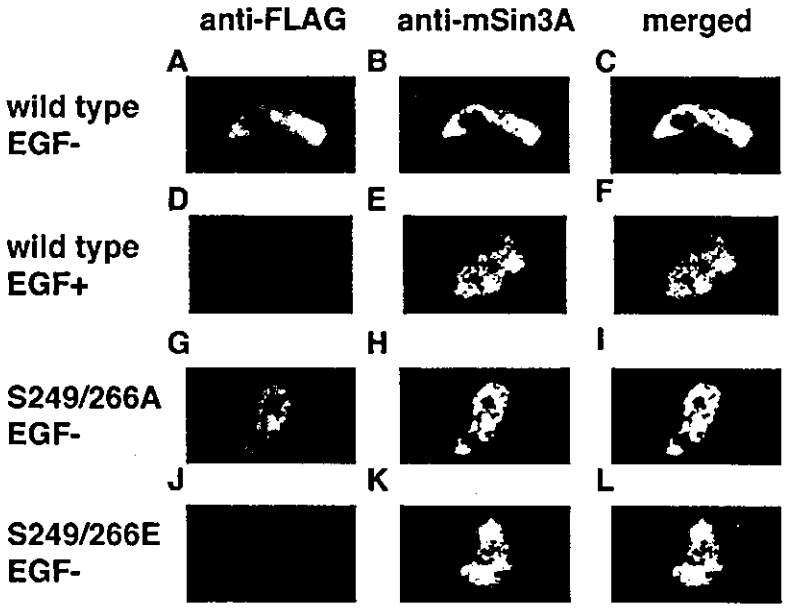

FIG. 3. Intranuclear translocation of AML1 induced by its phosphorylation. (A to F) COS-7 cells were transfected with FLAG-tagged wild-type AML1, together with ERK and PEBP2β, and incubated in the absence (A to C) or the presence (D to F) of EGF. The cells were treated with in situ nuclear-matrix preparations, and immunofluorescent staining was performed using the anti-FLAG antibody (A and D), the anti-mSin3A antibody (B and E), or both (C and F). (G to L) COS-7 cells were cotransfected with FLAG-tagged S249/266A (G to I) or S249/266E (J to L) with PEBP2β. The cells were treated with in situ nuclear matrix preparations, and immunofluorescent staining was performed using the anti-FLAG antibody (G and J), the anti-mSin3A antibody (H and K), or both (I and L).

AML1 or S249/266A, together with ERK, and then treated for 5 min with graded concentrations of EGF and harvested 10 or 30 min after the removal of EGF. In these experiments, we did not cotransfect PEBP2β into COS-7 cells to eliminate the effect of PEBP2β overexpression on protection of AML1 (7). The cells were cultured in the presence of phosphatase inhibitors to protect AML1 from dephosphorylation. The cell lysates were subjected to SDS-PAGE and Western blotting with the anti-FLAG antibody. As shown in Fig. 7, slowly migrating bands of wild-type AML1, which correspond to phosphorylated forms, were observed 10 min after the removal of EGF in an EGF dose-dependent manner (lanes 3 and 5). After 30 min, the amounts of unphosphorylated AML1 remained unchanged (lanes 4 and 6). Furthermore, S249/266A showed constant levels of expression, regardless of the incubation periods after EGF removal (lanes 7 and 8). These results indicate that unphosphorylated AML1 is stable upon EGF stimulation. In contrast, expression of the phosphorylated forms was markedly diminished at both concentrations of EGF, even in the presence of phosphatase inhibitors (lanes 4 and 6). These data suggest that ERK-dependent phosphorylation promotes proteasome-mediated degradation of AML1.

Analyses of the stability of AML1 in PEBP2β-deficient fibroblasts. To determine more explicitly a role for phosphorylation-dependent mSin3A interaction in the degradation of AML1, we established fibroblasts from PEBP2β-deficient embryos, which allowed us to eliminate the effect of endogenous PEBP2β on the protection of AML1 (7).

In embryonic fibroblasts from normal mice, we detected endogenous PEBP2β (Fig. 8A, lane 1). On the other hand, PEBP2β was not detected in PEBP2β-deficient fibroblasts (Fig. 8A, lane 2). First, we examined whether AML1 would undergo ERK-mediated phosphorylation and subsequent proteolytic degradation in these cells. We cotransfected wild-type AML1 and ERK into PEBP2β-deficient fibroblasts and stimulated the cells with EGF for 5 min. The cell lysates were analyzed by Western blotting. After 5 min of EGF stimulation, both phosphorylated and unphosphorylated AML1 were observed by Western blotting (Fig. 8B, lane 2). However, when we harvested the transfected cells after 30 min of EGF stimulation, there was a marked reduction in the amount of AML1 such that both forms of AML1 were barely detected (Fig. 8B, lane 3). When S249/266A was transfected into these cells together with ERK, followed by stimulation with EGF, neither the mobility shift nor the decrease in the amount of S249/266A was observed, regardless of EGF stimulation (Fig. 8B, lanes 4 to 6). These results suggest that AML1 is phosphorylated upon the activation of ERK in PEBP2β-deficient fibroblasts and that phosphorylated AML1 is degraded with the lapse of time after EGF stimulation.

Next, we tested the stability of the AML1 mutant that mimics the phosphorylated form in these cells. Wild-type AML1 and S249/266E were expressed at equivalent levels in PEBP2β-deficient fibroblasts when transfected in the presence of lactacystin, which strongly inhibits proteasome-mediated protein degradation (Fig. 8C, lanes 1 and 3). It is expected that AML1 is liable to undergo degradation in PEBP2β-deficient cells without proteolysis inhibition. In support of this, expression of wild-type AML1 and S249/266E noticeably decreased without lactacystin treatment (Fig. 8C, lanes 2 and 4). Furthermore, degradation induced by lactacystin removal was more prominent in S249/266E than in wild-type AML1, which was not

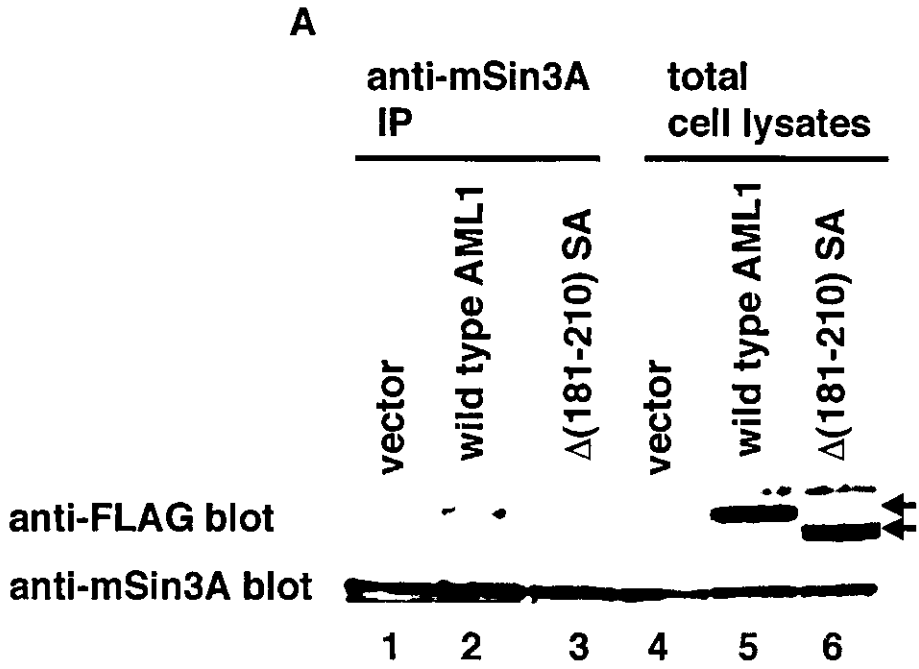

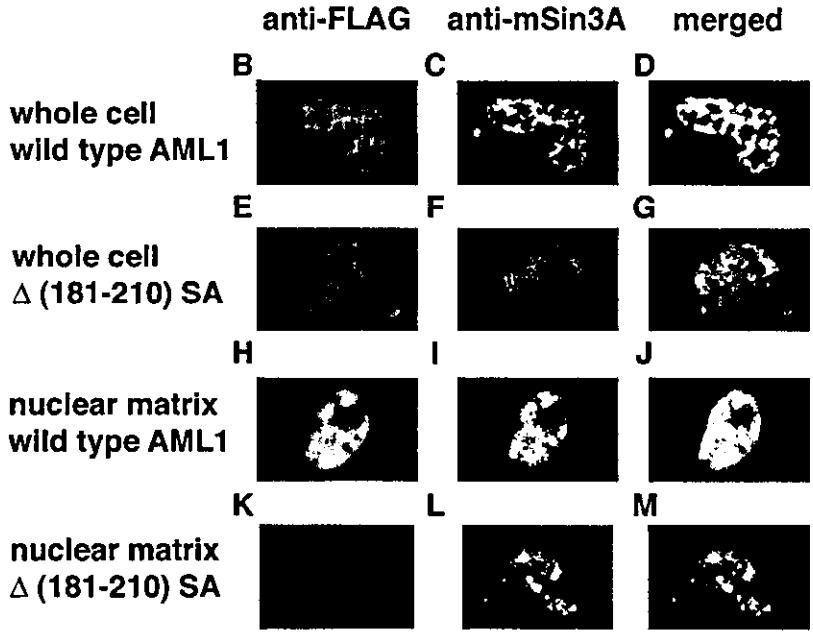

FIG. 4. The AML1 mutant lacking the interaction domain with mSin3A does not colocalize with mSin3A in the nuclear matrix. (A) COS-7 cells were cotransfected with pME18S, pME-FLAG-AML1, or pME-FLAG-Δ(181-210)SA with pME-PEBP2β and harvested. The cell lysates were precleared with protein G-Sepharose, mixed with anti-mSin3A antibody, and rotated for 2 h at 4°C. Then, mSin3A was recovered on protein G-Sepharose beads. The washed beads were subjected to SDS-PAGE, followed by Western blotting with anti-FLAG or anti-mSin3A antibody. Expression of each protein was monitored by using 60 μg of total cell lysates. Arrows indicate the wild type and mutant of AML1. (B to M) COS-7 cells were cotransfected with FLAG-tagged wild-type AML1 (B to D and H to J) or Δ(181-210)SA (E to G and K to M) with PEBP2β. The cells were treated with whole-cell (B to G) or in situ nuclear-matrix (H to M) preparations, and immunofluorescent staining was performed using the anti-FLAG antibody (B, E, H, and K), the anti-mSin3A antibody (C, F, I, and L), or both (D, G, J, and M).

distinct in COS-7 cells (Fig. 8C, lanes 2 and 4). These results suggest that phosphorylation-dependent degradation of AML1 is facilitated in PEBP2β-deficient cells.

Recapitulating phosphorylation-dependent degradation of AML1 in PEBP2β-deficient cells, we subsequently tested whether mSin3A can protect AML1 from degradation in these cells. We transfected wild-type AML1 or Δ(181-210)SA into the cells without EGF stimulation. As shown in Fig. 8D, ex-

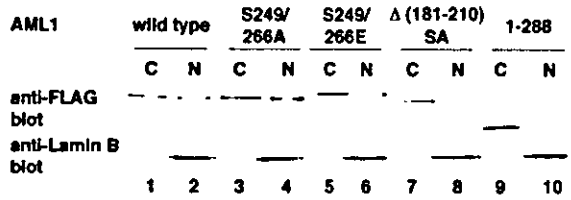

FIG. 5. Biochemical-fractionation assay of wild-type AML1 and AML1 mutants in COS-7 cells. COS-7 cells were transfected with pME-FLAG-AML1 (lanes 1 and 2), pME-FLAG-S249/266A (lanes 3 and 4), pME-FLAG-S249/266E (lanes 5 and 6), pME-FLAG-Δ(181-210)SA (lanes 7 and 8), or pME-FLAG-AML1 1-288 (lanes 9 and 10). Extract of the chromatin (15%) (lanes 1, 3, 5, 7, and 9) or 5% extract of the nuclear-matrix (lanes 2, 4, 6, 8, and 10) fraction was loaded in each lane. Western blot analyses were performed using the anti-FLAG and the anti-lamin B1 antibodies. C, chromatin; N, nuclear matrix.

pression of Δ(181-210)SA was much lower than that of wild-type AML1 regardless of lactacystin treatment in PEBP2β-deficient fibroblasts. These results suggest that mSin3A plays a key role in protecting AML1 from proteasome-mediated degradation and provide us with a potential mechanism for phosphorylation-induced degradation of AML1.

To address the relative contributions of PEBP2β to the stability of AML1 when AML1 is phosphorylated, we investigated whether the interaction between AML1 and PEBP2β would change when AML1 was phosphorylated. We transfected FLAG-tagged AML1 together with ERK and PEBP2β into COS-7 cells. When we stimulated the cells with EGF, we observed the shifted band of AML1 corresponding to the phosphorylated AML1 (Fig. 9, lane 3). When we immunoprecipitated FLAG-tagged AML1 with the anti-FLAG antibody, constant amounts of PEBP2β were coimmunoprecipitated regardless of EGF stimulation (Fig. 9, lanes 2 and 3). These

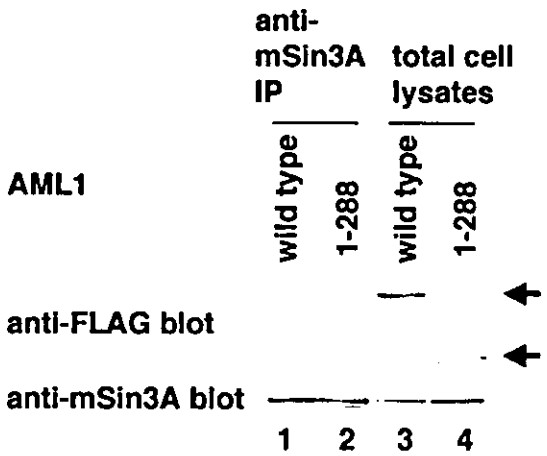

FIG. 6. Effect of a mutation in the nuclear-matrix attachment site of AML1 on interaction with mSin3A. COS-7 cells were transfected with pME-FLAG-AML1 (lane 1) or pME-FLAG-AML1 1-288 (lane 2) and harvested. The cell lysates were precleared with protein G-Sepharose, mixed with anti-mSin3A antibody, and rotated for 2 h at 4°C. Then, mSin3A was recovered on protein G-Sepharose beads. The washed beads were subjected to SDS-PAGE, followed by Western blotting with anti-FLAG or anti-mSin3A antibody. Expression of each protein was confirmed by using 30 μg of total lysates. Arrows, wild-type and mutant AML1.

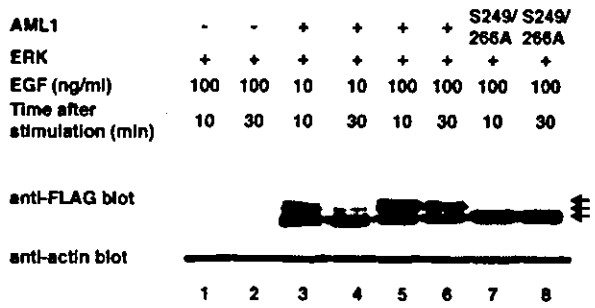

FIG. 7. Phosphorylated AML1 is degraded in a time-dependent manner in COS-7 cells. COS-7 cells were cotransfected with pME18S (lanes 1 and 2), pME-FLAG-AML1 (lanes 3 to 6), or pME-FLAG-S249/266A (lanes 7 and 8), together with pCMVMK; starved in medium containing 0.1% FCS; and treated for 5 min with 10 (lanes 3 and 4) or 100 (lanes 1, 2, and 5 to 8) ng of EGF per ml plus 10% FCS in the presence of 50 mM sodium fluoride as a phosphatase inhibitor. The cells were harvested after 10 (lanes 1, 3, 5, and 7) or 30 (lanes 2, 4, 6, and 8) min of EGF stimulation, and 30 μg of total cell lysates was subjected to SDS-PAGE, followed by Western blotting with the anti-FLAG or antiactin antibody. +, present; −, absent; arrows, phosphorylated and unphosphorylated AML1.

results indicate that the interaction between AML1 and PEBP2β does not change when AML1 is phosphorylated and that the degradation of phosphorylated AML1 is not due to loss of interaction with PEBP2β. These results argue that association with mSin3A, in addition to PEBP2β, is required for AML1 to exist stably in cells and that loss of interaction with mSin3A plays an important role in the degradation of phosphorylated AML1.

Transcriptional activities of S249/266E and Δ(181-210)SA mutants of AML1. We found that S249/266E and Δ(181-210)SA are dissociated from the corepressor mSin3A. These results suggest that the transcriptional activities of these mutants are higher than those of wild-type AML1. Therefore, we tested the transcriptional activities of these mutants in transcriptional-response assays.

When we cotransfected wild-type AML1, S249/266E, or Δ(181-210)SA into P19 cells in the presence of 10% FCS with the Tww-tk-Luc reporter, there was no significant difference between the transcriptional activities of wild-type AML1 and those of the mutants (data not shown). We showed the loss of stability of S249/266E and Δ(181-210)SA (Fig. 8C and D), and these results may explain the decrease in the transcriptional activities of the mutants. Furthermore, when transfected into COS-7 cells in the presence of 10% FCS, a significant proportion of wild-type AML1 is phosphorylated without EGF stimulation (data not shown). We therefore cotransfected wild-type AML1, S249/266E, or Δ(181-210)SA into COS-7 cells with Tww-tk-Luc reporter and created the cells with 0.1% FCS to eliminate the effect of FCS. In these experiments, S249/266E and Δ(181-210)SA showed higher transcriptional activities than wild-type AML1 (Fig. 10, lanes 3 and 4). These results are consistent with our findings that the mutants lose interaction with the corepressor mSin3A. Compared with S249/266E, Δ(181-210)SA showed reduced transcriptional activities. As shown in Fig. 8C and D, the expression of Δ(181-210)SA is lower than that of wild-type AML1 regardless of lactacystin treatment, although wild-type AML1 and S249/266E were ex-

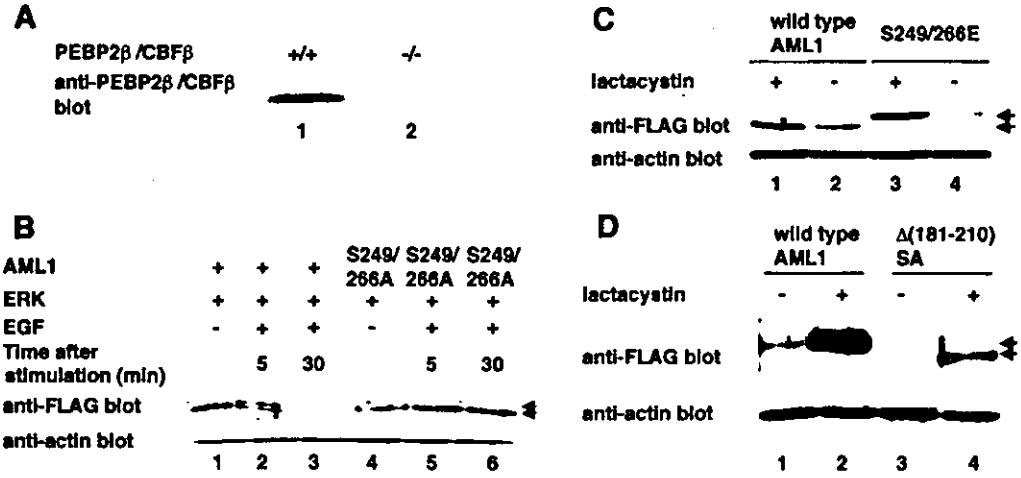

FIG. 8. Phosphorylated AML1 and the AML1 mutants lacking interaction with mSin3A are degraded by proteasome in PEBP2β-deficient fibroblasts. (A) Embryonic fibroblasts from normal mice (lane 1) or PEBP2β-deficient mice (lane 2) were lysed, and 30 μg of cell lysates were subjected to SDS-PAGE and Western blotting with anti-PEBP2β antibody. (B) PEBP2β-deficient fibroblasts were cotransfected with (+) pME-FLAG-AML1 (lanes 1 to 3) or pME-FLAG-S249/266A (lanes 4 to 6), together with pCMVMK. The cells were starved in medium containing 0.1% FCS overnight and treated for 5 min with 100 ng of EGF per ml plus 10% FCS (lanes 2, 3, 5, and 6) or left untreated (lanes 1 and 4). They were harvested, and 30 μg of cell lysates was subjected to SDS-PAGE and Western blotting with anti-FLAG or anti-actin antibody. The EGF-treated cells were harvested after 5 (lanes 2 and 5) or 30 (lanes 3 and 6) min of EGF stimulation. Arrows, phosphorylated and unphosphorylated AML1. (C) PEBP2β-deficient fibroblasts were transfected with pME-FLAG-AML1 or pME-FLAG-S249/266E. The cells were treated with 10 μM lactacystin (lanes 1 and 3) or left untreated (lanes 2 and 4) overnight and harvested; 30 μg of cell lysates was subjected to SDS-PAGE and Western blotting with anti-FLAG or anti-actin antibody. (D) PEBP2β-deficient fibroblasts were transfected with pME-FLAG-AML1 or pME-FLAG-Δ(181-210)SA. The cells were treated with 10 μM lactacystin (lanes 2 and 4) or left untreated (lanes 1 and 3) overnight and harvested; 30 μg of cell lysates was subjected to SDS-PAGE and Western blotting with anti-FLAG or anti-actin antibody. Arrows in panels C and D indicate wild-type and mutant AML1.

pressed at equivalent levels in the presence of lactacystin. These results suggest that the stability of Δ(181-210)SA is lower than that of S249/266E, and this may explain the reduction in the transcriptional activity of Δ(181-210)SA.

Transcriptional activity of AML1 following EGF stimulation. In the present study, we demonstrated that phosphorylated AML1 is prone to proteasome-mediated degradation. Thus, AML1 should exhibit decreased activity in transcriptional assays upon prolonged EGF stimulation. To confirm this, we investigated the change in transcriptional activity of AML1 following EGF stimulation. When we overexpressed AML1 and ERK with the Tww-tk-Luc reporter in COS-7 cells and harvested the cells after stimulation with 100 ng of EGF per ml for 15 min, we observed 10-fold induction of transcriptional activity (Fig. 11A, lane 2). On the other hand, we ob-

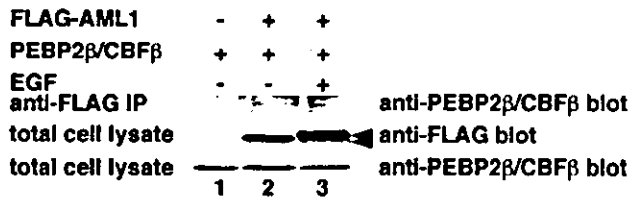

FIG. 9. Analyses of the interaction between phosphorylated AML1 and PEBP2β. COS-7 cells were transfected with pME18S (lane 1) or pME-FLAG-AML1 (lanes 2 and 3), together with pCMV-MK and pME-PEBP2β. The cells were treated for 5 min with EGF (lane 3) or left untreated (lanes 1 and 2) and harvested with lysis buffer. The cell lysates were precleared with protein G-Sepharose, mixed with anti-FLAG antibody, and rotated for 2 h at 4°C. Then, FLAG-AML1 was recovered on protein G-Sepharose beads. The washed beads were subjected to SDS-PAGE, followed by Western blotting with anti-PEBP2β antibody. Expression of each protein was confirmed by using 60 μg of total cell lysates. Arrows, phosphorylated and unphosphorylated AML1.

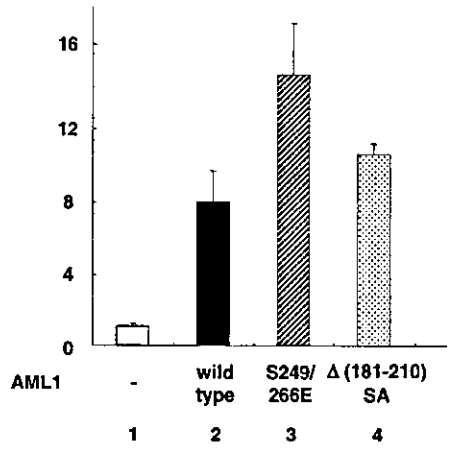

FIG. 10. Transcriptional activities of S249/266E and Δ(181-210)SA mutants of AML1. COS-7 cells were cotransfected with 500 ng of Tww-tk-Luc and 200 ng of pME18S (AML1, −), pME-FLAG-AML1 AML1, wild type), pME-FLAG-S249/266E, or pME-FLAG-Δ(181-210)SA as indicated. The cells were cultured in DMEM containing 0.1% FCS for 12 h after transfection and harvested. The means and standard deviations of the luciferase activities of AML1 and the mutants in two independent transfections are shown. We used the mean of the luciferase activities of the expression vector (pME18S) in two independent transfections as the control.

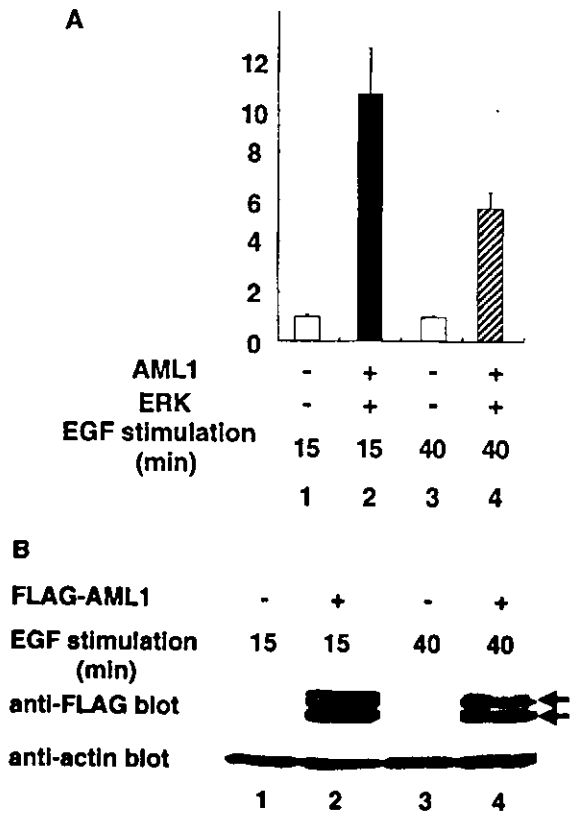

FIG. 11. Transcriptional activity of AML1 following EGF stimulation. (A) COS-7 cells were cotransfected with 500 ng of Tww-tk-Luc and 400 ng of pME18S (lanes 1 and 3) or 200 ng of pCMV-MK and pME-FLAG-AML1 (lanes 2 and 4). The cells were cultured in DMEM containing 0.1% FCS for 12 h after transfection. We harvested the cells after incubation in medium containing 100 ng of EGF per ml for 15 (lanes 1 and 2) or 40 (lanes 3 and 4) min. The means and standard deviations of the luciferase activities of AML1 in two independent transfections are shown. We used the mean of luciferase activities of the expression vector (pME18S) in two independent transfections as the control. (B) COS-7 cells were cotransfected with 500 ng of Tww-tk-Luc and 400 ng of pME18S (lanes 1 and 3) or 200 ng of pCMV-MK and pME-FLAG-AML1 (lanes 2 and 4). The cells were cultured in DMEM containing 0.1% FCS for 12 h after transfection. We harvested the cells after incubation in medium containing 100 ng of EGF per ml for 15 (lanes 1 and 2) or 40 (lanes 3 and 4) min; 30 μg of total cell lysates of the transfected cells was subjected to SDS-PAGE, followed by Western blotting with anti-FLAG or antiactin antibody. Arrows, phosphorylated and unphosphorylated AML1.

served only fivefold induction of transcriptional activity when we harvested the cells after 40 min of stimulation by EGF (Fig. 11A, lane 4). After 15 min of stimulation by EGF, we observed both phosphorylated (Fig. 11B, lane 2) and unphosphorylated (Fig. 11B, lane 2) forms of AML1 in Western blotting. After 40 min of stimulation by EGF, however, we observed a marked reduction in the amount of phosphorylated AML1 (Fig. 11B, lane 4). These results support the idea that degradation may cause decreased transcriptional activity of phosphorylated AML1 with prolonged EGF stimulation.

DISCUSSION

Phosphorylation-dependent regulation of AML1 functions is mediated by the interaction between AML1 and mSin3A. Transcriptional repression is regulated by several different mechanisms (4, 6). One of them involves the recruitment of corepressor complexes, many of which contain subunits that possess HDACs, to the target genes (32). HDACs act to deacetylate histones and thus convert chromatin into a repressive state (1). In the mSin3A-HDAC complex, mSin3A acts as a linker to transcription factors, such as Mad, p53, TEL, and Ikaros (14, 18, 25). The previous study showed that AML1 also interacts with mSin3A and that this interaction mediates repression of the p21 promoter by AML1 (21). However, it was not shown how the interaction between AML1 and mSin3A is regulated.

We demonstrated that mSin3A binds to AML1 when it is not phosphorylated and that mSin3A is released from phosphorylated AML1 upon activation of ERK. mSin3A is known to recruit class I HDACs (13). When associated with DNA, this complex can deacetylate chromatin and silence transcription. In the previous study, we showed that the transcription of TCRβ induced by AML1 is dependent on phosphorylation of AML1 and that the AML1 mutant cannot be phosphorylated, showing reduced transcriptional activity. Here, we revealed that this reduction is alleviated by treatment with TSA. This suggests that the reduced transcriptional activity of the unphosphorylated AML1 mutant is due to its interaction with mSin3A. We conclude that mSin3A suppresses AML1 transcriptional activity by linking AML1 to HDACs when AML1 is not phosphorylated and that AML1 released from mSin3A upon ERK-induced phosphorylation becomes active as a transcriptional activator. These results provide a novel mechanism by which extracellular stimuli convert inactive forms of transcription factors into active ones.

Intranuclear localization of AML1 is regulated by interaction with mSin3A. AML1 is a nuclear protein that is localized in the nuclear matrix (47). The in situ immunofluorescence study and the biochemical-fractionation assay demonstrated that wild-type AML1 translocates from the nuclear matrix, where mSin3A is located when it is phosphorylated, supporting our finding that AML1 dissociates itself from mSin3A upon phosphorylation. The deletion mutant of AML1 lacking the interaction domain with mSin3A translocates from the nuclear matrix without phosphorylation, and a mutation in the nuclear-matrix attachment site disrupts the interaction between AML1 and mSin3A. One plausible explanation for this observation is that the interaction of AML1 with mSin3A plays an important role in targeting to the nuclear matrix. This is also supported by our findings that the mutant of AML1 that mimics phosphorylated AML1 lacks its association with mSin3A and that it is released from the nuclear matrix. The previous studies showed that the carboxyl terminus of AML1 is also necessary for targeting to the nuclear matrix (3, 47). From these results, it is suggested that both the mSin3A interaction domain and the carboxyl-terminal domain of AML1 are necessary for its localization in the nuclear matrix.

The importance of the nuclear-matrix targeting in the function of AML1 is not clear. AML1 was shown to colocalize with a subset of hyperphosphorylated RNA polymerase II in the nuclear matrix, which suggests that the association with the nuclear matrix is necessary to support AML1 transcriptional activity (46). In that study, however, only a subset of AML1 was associated with RNA polymerase II in the nuclear matrix

whereas a significant amount of AML1 proteins was not. More recently, it was shown that targeting of AML1 to the nuclear matrix is required for the initiation of DNA replication (3). Our data raise the possibility that AML1 works as an active repressor when bound to mSin3A in the nuclear matrix. Once it is phosphorylated, transcriptional repression by AML1 may be abolished. Furthermore, AML1 released from the nuclear matrix may bind to the other regulatory elements in the chromatin and activate gene transcription. Further mechanisms that dictate AML1 activation after mSin3A release remain to be elucidated.

Regulation of the stability of AML1 by phosphorylation. The previous study reported that heterodimerization with PEBP2β protects AML1 from proteasome-mediated degradation (7). However, our data indicate that phosphorylated AML1 is degraded in a time-dependent manner in COS-7 cells that contain endogenous PEBP2β. These results raise the possibility that some proteins other than PEBP2β may protect unphosphorylated AML1 from degradation and that their loss of interaction may cause degradation of phosphorylated AML1. Our analyses of the AML1 mutant lacking the domain interacting with mSin3A support the ability of mSin3A to protect AML1 from degradation. These results provide a novel regulatory mechanism that governs the stability of AML1.

In PEBP2β-deficient fibroblasts, both phosphorylated and unphosphorylated AML1 were observed by Western blotting after 5 min of EGF stimulation (Fig. 8B, lane 2), and unphosphorylated AML1 was completely degraded after 30 min of EGF stimulation (Fig. 8B, lane 3). It is supposed that unphosphorylated AML1 is phosphorylated and degraded during the 30 min after EGF stimulation. In COS-7 cells, both phosphorylated and unphosphorylated forms of AML1 are observed after 30 min of EGF stimulation (Fig. 7, lanes 4 and 6). This discrepancy is due to the fact that COS-7 cells contain endogenous PEBP2β, which protects AML1 from degradation.

A mechanism for regulation of AML1 activation induced by its phosphorylation. Recently, it was shown that phosphorylation of the transcription factor Elk-1 in response to ERK activation induces recruitment of the mSin3A-HDAC1 complex and repression of transcription from its target promoters (45). In our study, phosphorylation of AML1 induced the release of AML1 from mSin3A and enhanced AML1 transcriptional activity. Furthermore, phosphorylation regulates the stability of AML1 via interaction with mSin3A, manifested by the fact that phosphorylated AML1 is subjected to proteasome-mediated degradation. Thus, one additional role of corepressor release from AML1 may be to set a ceiling on the degree and duration of AML1 activation in response to cytokine and growth factor stimuli.

In summary, our studies have identified a novel mechanism by which ERK-induced phosphorylation regulates AML1 function. These findings will contribute to elucidation of the leukemogenic mechanisms derived from the dysfunction of AML1.

ACKNOWLEDGMENTS

We thank M. Ohki for providing us with AML1 cDNA.

This work was supported in part by grants-in-aid from the Japan Society for the Promotion of Science; the Ministry of Education, Culture, Sports, Science and Technology; and the Ministry of Health, Labor and Welfare.

REFERENCES

1. **Ayer, D. E.** 1999. Histone deacetylases: transcriptional repression with SINers and NuRDs. Trends Cell Biol. **9**:193–198.
2. **Bruhn, L., A. Munnerlyn, and R. Grosschedl.** 1997. ALY, a context-dependent coactivator of LEF-1 and AML-1, is required for TCRα enhancer function. Genes Dev. **11**:640–653.
3. **Chen, L. F., K. Ito, Y. Murakami, and Y. Ito.** 1998. The capacity of polyomavirus enhancer binding protein 2αB (AML1/Cbfa2) to stimulate polyomavirus DNA replication is related to its affinity for the nuclear matrix. Mol. Cell. Biol. **18**:4165–4176.
4. **Cowell, I. G.** 1994. Repression versus activation in the control of gene transcription. Trends Biochem. Sci. **19**:38–42.
5. **Golub, T. R., G. F. Barker, S. K. Bohlander, S. W. Hiebert, D. C. Ward, P. Bray-Ward, E. Morgan, S. C. Raimondi, J. D. Rowley, and D. G. Gilliland.** 1995. Fusion of the TEL gene on 12p13 to the AML1 gene on 21q22 in acute lymphoblastic leukemia. Proc. Natl. Acad. Sci. USA **92**:4917–4921.
6. **Herschbach, B. M., and A. D. Johnson.** 1993. Transcriptional repression in eukaryotes. Annu. Rev. Cell Biol. **9**:479–509.
7. **Huang, G., K. Shigesada, K. Ito, H. J. Wee, T. Yokomizo, and Y. Ito.** 2001. Dimerization with PEBP2β protects RUNX1/AML1 from ubiquitin-proteasome-mediated degradation. EMBO J. **20**:723–733.
8. **Imai, Y., M. Kurokawa, K. Izutsu, A. Hangaishi, K. Maki, S. Ogawa, S. Chiba, K. Mitani, and H. Hirai.** 2001. Mutations of the Smad4 gene in acute myelogeneous leukemia and their functional implications in leukemogenesis. Oncogene **20**:88–96.
9. **Imai, Y., M. Kurokawa, K. Izutsu, A. Hangaishi, K. Takeuchi, K. Maki, S. Ogawa, S. Chiba, K. Mitani, and H. Hirai.** 2000. Mutations of the AML1 gene in myelodysplastic syndrome and their functional implications in leukemogenesis. Blood **96**:3154–3160.
10. **Imai, Y., M. Kurokawa, K. Tanaka, A. D. Friedman, S. Ogawa, K. Mitani, Y. Yazaki, and H. Hirai.** 1998. TLE, the human homolog of Groucho, interacts with AML1 and acts as a repressor of AML1-induced transactivation. Biochem. Biophys. Res. Commun. **252**:582–589.
11. **Ishida, N., M. Kitagawa, S. Hatakeyama, and K. Nakayama.** 2000. Phosphorylation at serine 10, a major phosphorylation site of p27(Kip1), increases its protein stability J. Biol. Chem. **275**:25146–25154.
12. **Kitabayashi, I., A. Yokoyama, K. Shimizu, and M. Ohki.** 1998. Interaction and functional cooperation of the leukemia-associated factors AML1 and p300 in myeloid cell differentiation. EMBO J. **17**:2994–3004.
13. **Knoepfler, P. S., and R. N. Eisenman.** 1999. Sin meets NuRD and other tails of repression. Cell **99**:447–450.
14. **Koipally, J., A. Renold, J. Kim, and K. Georgopoulos.** 1999. Repression by Ikaros and Aiolos is mediated through histone deacetylase complexes. EMBO J. **18**:3090–3100.
15. **Kunkel, T. A., J. D. Roberts, and R. A. Zakour.** 1987. Rapid and efficient site-specific mutagenesis without phenotypic selection. Methods Enzymol. **154**:367–382.
16. **Kurokawa, M., K. Mitani, K. Irie, T. Matsuyama, T. Takahashi, S. Chiba, Y. Yazaki, K. Matsumoto, and H. Hirai.** 1998. The oncoprotein Evi-1 represses TGF-β signalling by inhibiting Smad3. Nature **394**:92–96.
17. **Kurokawa, M., T. Tanaka, K. Tanaka, S. Ogawa, K. Mitani, Y. Yazaki, and H. Hirai.** 1996. Overexpression of the AML1 proto-oncoprotein in NIH3T3 cells leads to neoplastic transformation depending on the DNA-binding and transactivational potencies. Oncogene **12**:883–892.
18. **Laherty, C. D., W. M. Yang, J. M. Sun, J. R. Davie, E. Seto, and R. N. Eisenman.** 1997. Histone deacetylases associated with the mSin3 corepressor mediate mad transcriptional repression. Cell **89**:349–356.
19. **Levanon, D., R. E. Goldstein, Y. Bernstein, H. Tang, D. Goldenberg, S. Stifani, Z. Paroush, and Y. Groner.** 1998. Transcriptional repression by AML1 and LEF-1 is mediated by the TLE/Groucho corepressors. Proc. Natl. Acad. Sci. USA **95**:11590–11595.
20. **Lutterbach, B., and S. W. Hiebert.** 2000. Role of the transcription factor AML-1 in acute leukemia and hematopoietic differentiation. Gene **245**:223–235.
21. **Lutterbach, B., J. J. Westendorf, B. Linggi, S. Isaac, E. Seto, and S. W. Hiebert.** 2000. A mechanism of repression by acute myeloid leukemia-1, the target of multiple chromosomal translocations in acute leukemia. J. Biol. Chem. **275**:651–656.
22. **Maciejewski, P. M., F. C. Peterson, P. J. Anderson, and C. L. Brooks.** 1995. Mutation of serine 90 to glutamic acid mimics phosphorylation of bovine prolactin. J. Biol. Chem. **270**:27661–27665.
23. **Mitani, K., S. Ogawa, T. Tanaka, H. Miyoshi, M. Kurokawa, H. Mano, Y. Yazaki, M. Ohki, and H. Hirai.** 1994. Generation of the AML1-EVI-1 fusion gene in the t(3;21)(q26;q22) causes blastic crisis in chronic myelocytic leukemia. EMBO J. **13**:504–510.
24. **Miyoshi, H., K. Shimizu, T. Kozu, N. Maseki, Y. Kaneko, and M. Ohki.** 1991. t(8;21) breakpoints on chromosome 21 in acute myeloid leukemia are clustered within a limited region of a single gene, AML1. Proc. Natl. Acad. Sci. USA **88**:10431–10434.